SOLID BIOMASS GASIFICATION FOR FUEL CELLS

A. Heinzel,
K. Friedrich, V. Hacker, H. Fuchs, R. Fankhauser
O. Simon, G. Beckmann
J. Roes, R. Wolters

Fraunhofer Institute for Solar Energy Systems
Technical University of Graz
Austrian Electricity Bord
University of Duisburg

Contract JOR3-CT96-0105

PUBLISHABLE REPORT

1. September 1996 to 18. February 1999

Research funded in part by
THE EUROPEAN COMMISSION
in the framework of
the Non Nuclear Energy Programme
JOULE III

Abstract

The gasification of woody biomass leads to a lean gas with a hydrogen content of 20 - 25%. Within the project the partners investigated the feasibility of usage of woodgas to generate electricity and heat by fuel cells. The main subjects of investigations were

- to evaluate the availability of woody biomass in Austria
- optimisation of gasification with respect to a clean and hydrogen rich gas mixture
- the experimental investigation of different gas clean-up processes
- to define the requirements of the different types of fuel cells with respect to gas purity
- and to perform overall plant simulations.

Experiments on gas purification were carried out with respect to

- catalytic tar removal
- the sponge iron process
- CO-shift conversion
- hydrogen separation by Palladium-membranes
- CO_2-scrubbing with subsequent methanisation of CO and CO_2

Several suitable combinations of gasification and purification processes with different fuel cells were defined. These overall processes were simulated with respect to mass and energy balances, the overall efficiency was calculated.

These combinations were

- gasification of predryed wood with air in a fluidized bed reactor
- the sponge iron process and SOFC
- two chains for generation of pure hydrogen by catalytic tar removal, CO-shift and as last step either the Palladium membrane of scrubbing plus methanisation.

As result, an overall electrical efficiency of the conversion of biomass to fuel for fuel cells of about 25 % was calculated. An exception is the simplest process, the combination of a gasifier with dust and tar removal and with the high temperature fuel cell SOFC. Thus, if hot gas clean up for removal of dust and tar is feasible, the combination with high temperature fuel cells (SOFC or MCFC) is an attractive process.

Partnership

Partner	Name	Addess
Fraunhofer Institute for Solar Energy Systems	Angelika Heinzel	Oltmannstr. 5 79100 Freiburg Deutschland
Austrian Electricity Bord	Otto Simon	Am Hof 6A 1011 Wien Österreich
Preussag Noell KRC	Michael Mayer	Alfred-Nobel-Str. 20 97080 Würzburg Deutschland
Technical University of Graz	Prof. Kurt Friedrich	Krenngasse 37 8010 Graz Österreich
University of Duisburg	Jürgen Roes	Lotharstr. 1 47057 Duisburg Deutschland

Objectives

The superior project objective is to design an electricity generating plant based on woody biomass as a fuel, using a gasifier, an upgrading and purification system and a fuel cell. This complete conversion line is investigated within a feasibility study, some key components of the gas treatment are experimentally verified. Specifications of biomass and the gasification process are given by the Austrian Electricity Board and the Preussag Noell GmbH, the experimental programme on gas purification is carried out by the Technical University of Graz, the University of Duisburg and the Fraunhofer Institute for Solar Energy Systems ISE. The investigated process is shown in figure 1. The collective experiences are used to design an optimised power plant.

The results are a good basis of knowledge for demonstration plants to be planned, designed and constructed.

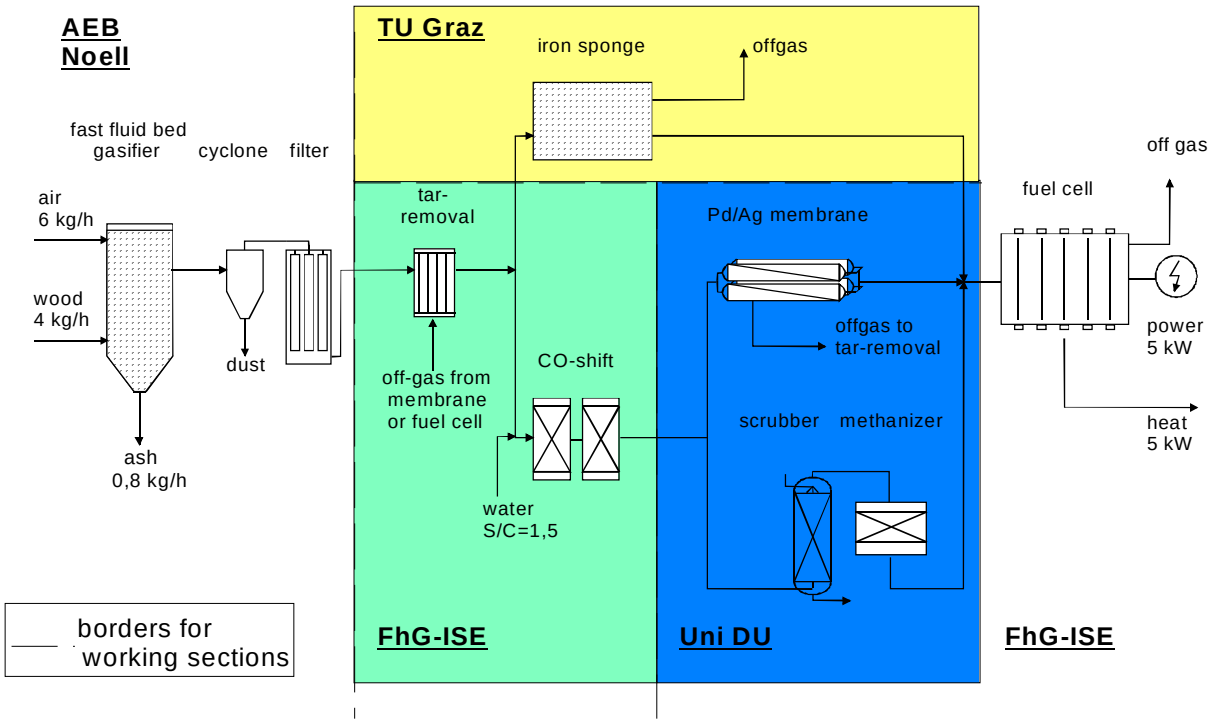

Figure 1: Schematic drawing of the investigated process

Technical description

1. Introduction

Fuel cell technology and the gasification of wood are technologies which are environmental friendly and efficient, but the state of the art still requires R&D efforts. In this project, a contribution to the promotion of both technologies is made by preparing a feasibility study starting from the availability of wood in Austria, considering various types of gasifiers, investigating different gas clean-up processes and collecting the available data on gas purity requirements of the different types of fuel cells.

The main requirements for a complete plant for conversion of biomass into hydrogen as a fuel for a fuel cell are efficiency, low emission levels and cost.

2. The availability of wooden biomass in Austria

In 1993 the wood supply in Austria was approx. 20 mio. m^3 (without imports). From this quantity 59% (11.8 mio. m^3) were structural timber, 22% (4.4 mio. m^3) fire wood, **13% (2.7 mio. m^3) residual wood+bark+hogged wood from forest** and 6% (1.1 mio. m^3) reused wood.

The national wood resources, stored in the Austrian forests, are approx. 972 mio m^3. Due to the fact that over the last years only 2/3 of the annual growth (31 mio. m^3) has been harvested, there is an capacity of approx. 57 mio. m^3 wood that could be yielded without damaging the forest stock.

An Austrian study estimates that 3,3 mio m^3 of this surplus could be used each year without decreasing the stock on the longterm (in order not to cut the whole quantity at once). Assuming that the biomass is used in the same manner than now **430 000 m^3** (equiv. 13 %) of this biomass are **available** for energetic use.

Preparation and logistic of harvesting

The activities necessary for making wood available for energetical utilisation are: forest maintenance, harvesting and transport (approx. 40 km). For these activities a total energy consumption of approx. 200 MJ/m^3 wooden biomass is required. Thus, considering the energy content of biomass (Hu=7,740 MJ/m^3), only **2.66%** of it is used for preparation and transport. Based on the **transport radius of approx. 40 km**, the biomass power plant can achieve a **thermal power of 10MW_{th}.**
Figure 2 shows the forest distribution in Austria. Some possible locations for the biomass power plant are Liezen, Mürzzuschlag and Obdach.

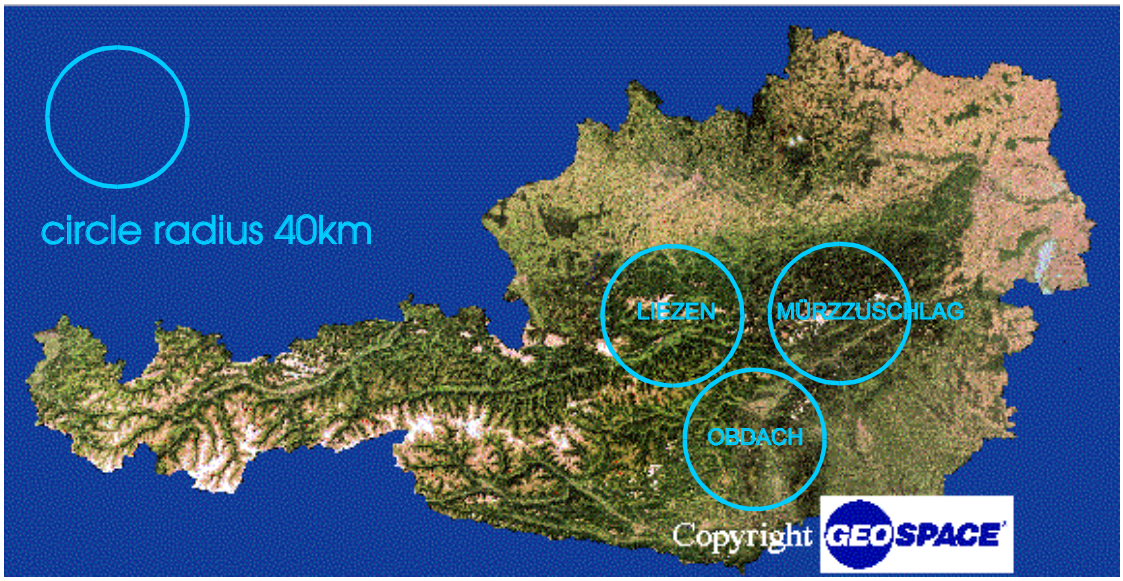

Figure 2: Forest distribution in Austria

Properties of selected biomass

	Proper -ties	***Unit***	***Wood*** *70%conifers 30% deciduous*	***Bark***	***rec. Value*** *50%conifers 30%bark 20% deciduous*	***Remarks***
calorific value LHV	water content w=30 %	[MJ/kg] [MJ/m^3]	12.36	12.76	**12.5** **7,740**	wood OeNORM M7231, bark acc. to DIN 51900[1)]
combustion value HHV	w=30 %	[MJ/kg]	13.32	13.54	**13.4**	wood OeN M7231, bark according to DIN 51900[1)]
solid density	w=30 %	[kg/m^3]	720	580	**680**	recommended value
spreading density, wood-chips W30 + Bark	w=30 %	[kg/m^3]	250	230	**240**	wood chips S200 OeNORM M7133
wood chips G100	coarse-grain	[mm]			**250x63**	OeNORM M7133
wood chips G50	coarse-grain	[mm]			**120x50**	OeNORM M7133
wood chips G30	coarse-grain	[mm]			**85x30**	OeNORM M7133

CHEMICAL COMPOSITION[1)]

carbon C	raw/wf	[weight%]	50.88 [48.8-52.2] (50.3waf)	51.57 [48.7-54.2]	**51.09**	Perkin Elmer 'Elementary-analyser 2400 CHN', (OeNORM B3011)
hydrogen H	raw/wf	[weight%]	5.62 [4.3-5.66] (6.14waf)	5.07 [4.33-6.10]	**5.46**	Perkin Elmer 'Elementary-analyser 2400 CHN.' (OeN B3011)
oxygen O	raw/wf	[weight%]	43.37 [42.5-46.1] (43.5waf)	42.87 [38.3-46.5]	**43.22**	(difference to 100) (OeN B3011)
nitrogen N	raw/wf	[weight%]	0.11 [0.06-0,31]	0.42 [0.35-1.43]	**0.203**	Perkin Elmer 'Elementary-analyser 2400 CHN'
sulphur S	raw/wf	[weight%]	0,01	0,05	**0.022**	Hi-temp. Combust. Wagner
chlorine Cl	raw/wf	[weight%]	0.01	0.02	**0.013**	Combustion Schoeninger
fluorine F	raw/wf	[weight%]			**n.a.**	
ash (A)	raw/wf	[weight%]	0.5 (0.2-0.4)	4 (1.0-9.0)	**1.55**	according to DIN 51719 (OeN B3011)
volatile components	raw/waf	[weight%]	85.0-88.0	n.a.	**n.a.**	OeN B3011
coke coal	raw	[weight%]	n.a.	n.a.	**n.a.**	
lead Pb	raw/wf	[ppm]	0.97 (0.4)[2]	28.15 (4.0)[2]	**9.12**	AAS Perkin Elmer 5000
cadmium Cd	raw/wf	[ppm]	0.21 (0.35)[3]	0.79 (0.6)[2]	**0.38**	AAS Perkin Elmer 5000
chromium Cr[4]	raw/wf	[ppm]	2.4 (0.44-0.51)[3]	5	**3.0**	
nickel Ni[3]	raw/wf	[ppm]	0.388 [0.28-0.64]	n.a.	**n.a.**	recommended value
mercury Hg	raw/wf	[ppm]	0.01	0.01 (0.04)[2]	**0,01**	AAS Perkin Elmer 503
zinc Zn	raw/wf	[ppm]	11 (22)[3]	90	**35**	
tin Sn	raw/wf	[ppm]	n.a.	n.a.	**n.a.**	

ASH MELTING TEMPERATURES[1)]					
Sinter point SB	[°C]	1180	1270	**1180-1270**	heating microscope
Softening point EP	[°C]	1470	1400	**1400-1470**	heating microscope
Hemisphere Temp. HP	[°C]	1600	1440	**1440-1600**	heating microscope
Melting point FP	[°C]	1640	1480	**1480-1640**	heating microscope
ASH COMPOSITION[1)]					
CO_2	[weight%]	21.6	13.7	**19.2**	method Scheibler
SO_3	[weight%]	1.1	1.2	**1.13**	Fusion with aqua regia
Cl	[weight%]	0.1	0.1	**0.10**	extraction in water
P_2O_5	[weight%]	3.3	1.8	**2.85**	ICP
SiO_2	[weight%]	21.1	25.5	**22.42**	ICP
Fe_2O_3	[weight%]	1.1	2.0	**1.37**	ICP
Al_2O_3	[weight%]	1.3	2.8	**1.75**	ICP
CaO	[weight%]	32.7	36.5	**33.84**	ICP
MgO	[weight%]	3.2	2.7	**3.05**	ICP
Na_2O	[weight%]	0.2	0.3	**0.23**	ICP
K_2O	[weight%]	9.4	4.7	**7.99**	ICP

Table 1: List of parameter / inputs EU-project [1)Hofbauer, 1994, 2) Schmidt, 1996, 3) Braun, 1992, 4) Kasser, 1994]
(n.a.= not acknowledged, raw=raw material, waf=water and ash-free, wf=water-free)

The ash-disposal has to be completed according to laws on soil protection, which are differing in each Austrian state.

Economical aspects

Biomass has no market price. A comparison of fuel prices (dated 1989) reveals that only bark, but not wood chips, has lower costs than fossil fuels. These costs will be updated 1999.

	[ECU /m^3]	[kg/m^3]	**Free boiler** [ECU /1000kg]	**Extra charges for fuel**	**Free burner** [ECU /1000kg]	[GJ /1000kg]	**Fuel** [ECU/GJ]
Bark coarse (53% H_2O)	2.19	370	11.84	5 %	12.43	7.77	1.60
Hogged wood (20% H_2O)	18.27	220	93.00	5 %	97.65	14.47	6.75
Hogged wood (30% H_2O)	14.61	250	67.20	5 %	70.56	12.36	5.71
Straw	-	235	73.07	3 %	75.26	14.97	5.03
Hard coal	-	-	97.18	3 %	100.10	28.47	3.52

*) incl. ECU 2,19 /m^3 transport costs for 40km **) 1ECU=öS13,685

Table 2: Comparison of fuel costs

Considering the barriers from legislation, ecology and technology, the most promising prospects regarding the use of biomass for energy production are: by-products of the wood-prelucration industry, fire wood, pruning from parks, orchard wood-cutting and wood-chips.
Due to the fact that only 2/3 of the annual growth of forests is presently used, we expect an increase of the technical utilisation potential from 116PJ (total biomass) used in 1994 to usable 200 PJ in 1999.

3. Gasification

For gasification of biomass, various fixed bed reactor types, fluidized bed and circulating fluidized bed gasifiers are known. With respect to the design of a smaller capacity, the following notable features should be considered:

- atmospheric gasifiers are favourable for smaller reactors, < 30 MWe, especially due to the high cost of the complex feeding system for pressurized gasifiers
- reactor design and gasification temperature influence the product gas composition, especially the tars, hydrocarbons and the char, high temperature favours the cracking.

In Table 3, some relevant data for various gasifiers are summarised.

	reaction temp.	exit gas temp.	tars	particul ates	turn-down	scalabi-lity	max. size [t/h]	Min. size [t/h]
fixed bed								
downdraft	1000	800	v.low	medium	good	poor	0,5	0,1
updraft	1000	250	v.high	medium	good	good	10*	1
cross current	900	900	v.high	high	fair	poor	1	0,1
fluid bed								
single reactor	850	800	fair	high	good	good	10*	1
fast fluid bed	850	850	low	v.high	good	v.good	20*	2
circulating bed	850	850	low	v.high	good	v.good	20*	2
entrained bed	1000	1000	low	v.high	poor	good	20*	5
twin reactor	800	700	high	fair	fair	good	10*	2
moving bed								
multiple hearth	700	600	high	low	poor	good	5	1
horizontal moving bed	700	600	high	low	fair	fair	5	1
sloping hearth	800	700	low	low	poor	fair	2	0,5
srew/auger kiln	800	700	high	low	fair	fair	2	0,5
other								
rotary kiln	800	800	high	high	poor	fair	10*	2
cyclone reactor	900	900	low	v.high	poor	fair	5	1

* current maxima but capable of scaling up to larger capacities

Table 3: Typical gasifier features

Figure 3 shows the concentrations of H_2, CO, CO_2 and CH_4 in an extended temperature range. The results show that high H_2 yields can be achieved under fluidized bed conditions.

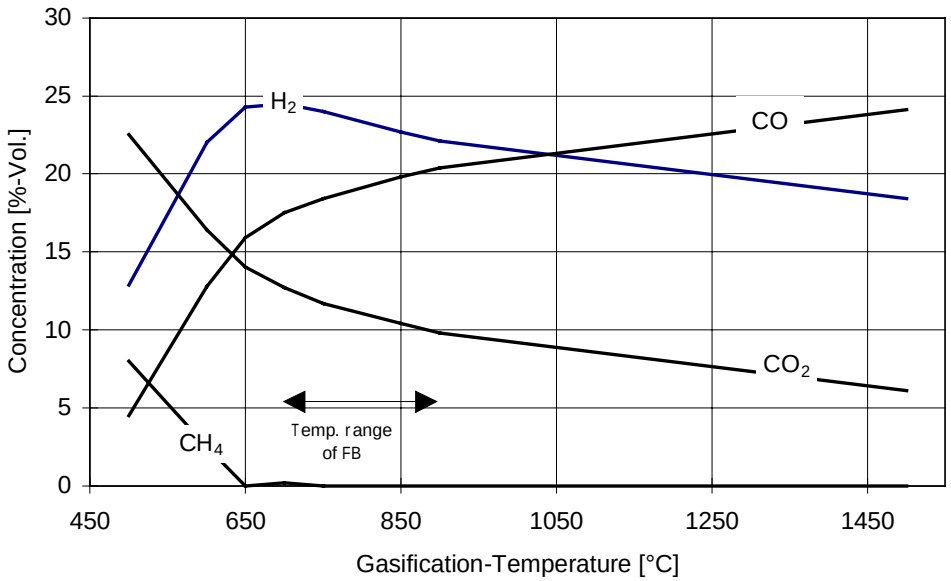

Figure 3 - Concentration of CH_4, CO, CO_2 and H_2 as a function of the gasification temperature

Resulting from the wood composition given in table 1, the gasifier gas will contain certain levels of impurities, as depicted in figure 4.

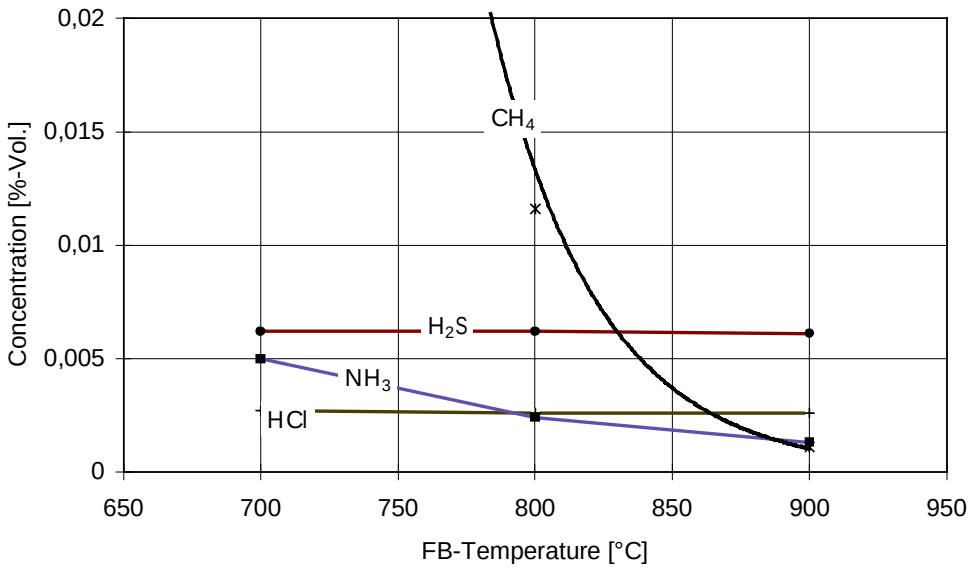

Figure 4 - Concentration of CH_4, HCl, H_2S and NH_3 as a function of the fluidized bed (FB) temperature

The most critical component is H_2S acting as catalyst poison for the subsequent catalytic gas purification processes.

4. Gas Purification

For all processes for generating electricity from gasifier gas, dust and tar must be removed. Usually, a scrubbing process with water is chosen, leading to a loss of heat and polluted waste water. Therefore a lot of efforts are undertaken to realise hot gas clean up systems, but the simultaneous removal of dust and tar at gasification temperature are still a challenge.

For this project, a dust free gas was assumed to be available, the complex composition of real tars was simulated by using aromatic tar model substances.

4.1. Tar/oil removal

The targeted experimental approach was to investigate catalytic processes for conversion of suitable tar model compounds. Aromatic species were chosen as model compounds as most tar species consist of polycondensed aromates and the suitability of the respectively tested catalyst/catalytic conversion process can be proven over the rate limiting decomposition of the aromatic structure into aliphatic fragments. The desirable reaction chain of course is to remove the hydrocarbons completely and to generate hydrogen and CO/CO_2.

Among the various catalytic processes to be taken into account steam reforming seems to be the most significant one because the gasification product gas principally includes much more water vapour than it is needed for a complete reforming, e.g. for naphthalene, according to

$$C_8H_{10} + 8\ H_2O \rightarrow 8\ CO + 13\ H_2$$

Catalytic reforming proceeds at temperatures between 500 and 1000°C over nickel or, between 500 and 850°C, over platinum catalysts. However, although nickel is the more usual catalytic material it is more sensitive against H_2S than platinum as long as reducing conditions are maintained.

For that purpose, a reactor was placed in a furnace for experiments in the temperature range from 500 to 1000 °C. A synthetic gasifier gas was used, the aromatic tar model component added by means of a saturiser. Additionally, small amounts of H2S could be added in order to investigate catalyst poisoning. Analysis of the product gas is carried out by FID for organic compounds in the hot and humid gas stream and after cooling down by NDIR-spectroscopy for the gases CO, CO_2, CH_4. Hydrogen cannot be detected by the available analytical equipment and has to be calculated as a balance. The total gas flow is measured by a gas meter.

A screening of commercially available catalysts was carried. All catalysts were crushed to a size of approximately 2 mm and placed between layers of quartz sand, after first experiments with benzene (poisonous substance) and naphtalene (solid at room temperature), finally toluene was chosen as tar model substance being easy to handle.

compound	gas composition, humid [Vol. %]	gas composition, dry [Vol.-%]
CO	8,2	11,9
CO_2	8,2	11,9
H_2	7,9	11,4
N_2	44,5	63,8
H_2O	30,2	-
toluene	1	1

Table 4: Gas composition for tar removal experiments

catalyst	chemical composition	physical properties
G-88 S	3 - 4 wt% NiO 13 - 15 wt% MoO_3 1-1,5 wt% P carrier: Al_2O_3	extrusions with a diameter of 3 mm bulk density approx. 0,6 kg/l side crush strength approx. 9 kg surface area 200 - 300 m^2/g pore volume > 29,2 A: 0,7 - 0,8 cm^3/g
T-4374	6 wt% Ni 0,3 wt% K carrier: magnesite	spheres with a diameter of 18 - 20 mm 1,5 kg/l bulk density crush strength approx. 100 kg
G-90B	Ni carrier: Al_2O_3	Raschig rings (16 x 10 x 8 mm)
G-31K	Ni, Pd carrier: Al_2O_3	spheres, 20mm diameter
G-133D	Pd carrier: Al_2O_3	spheres, ∅3-5 mm
K-0140	Pt carrier: Al_2O_3	cylinders, ∅3 x 3 mm

Table 5: Data of the catalysts

The catalyst G-88 S showed an insufficient conversion of toluene, the maximum level which could be achieved in the experiments was 40%, for G-133 D 800°C are required for a conversion rate of 90%.Thus, these two catalysts are not suitable for catalytic tar removal. But the catalysts T-4374 and G-90B are efficient catalysts for this purpose. For all measurements with the two catalysts T-4374, G-90B and K-0140, a complete conversion of toluene can be achieved at temperatures above 650°C, the methane content is low (below 1 Vol.-%) and a formation of carbon does not occur. The catalyst G 31 K also shows complete toluene conversion and a gas composition according to the thermodynamic equilibrium without carbon formation. Due to the high temperature stability up to 1200 °C this catalyst seems to be especially suitable for tar conversion and is one candidate for further investigations with sulfur containing educt gases.

As one typical example, the experimental results for catalyst G 90B are depicted in figure 5.

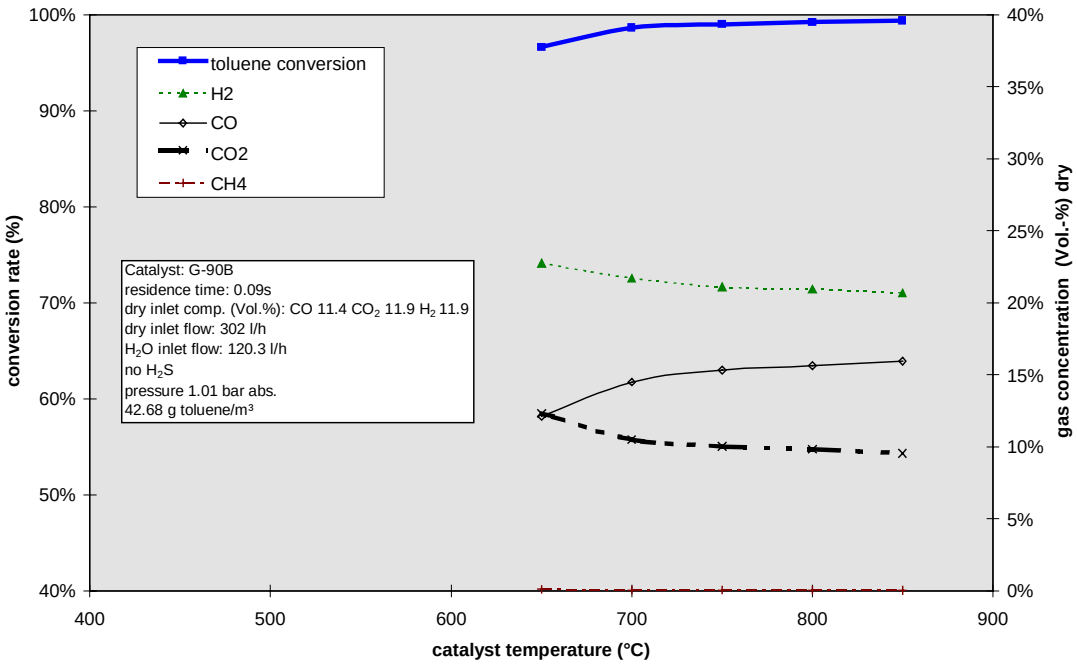

Figure 5: Gas composition and toluene conversion rate for catalyst G-90B in dependence on reaction temperature

Measurements with H_2S

The H_2S-content of the gas mixture (dry) was adjusted to 100 ppm. As noble metal catalysts are known to be more stable with respect to catalyst poisons, these catalysts were investigated at first. As example, the result of a measurement with the catalysts T-4374 is shown, a comparison of the toluene conversion rate without and with H_2S in the gas mixture is shown in figure 6.

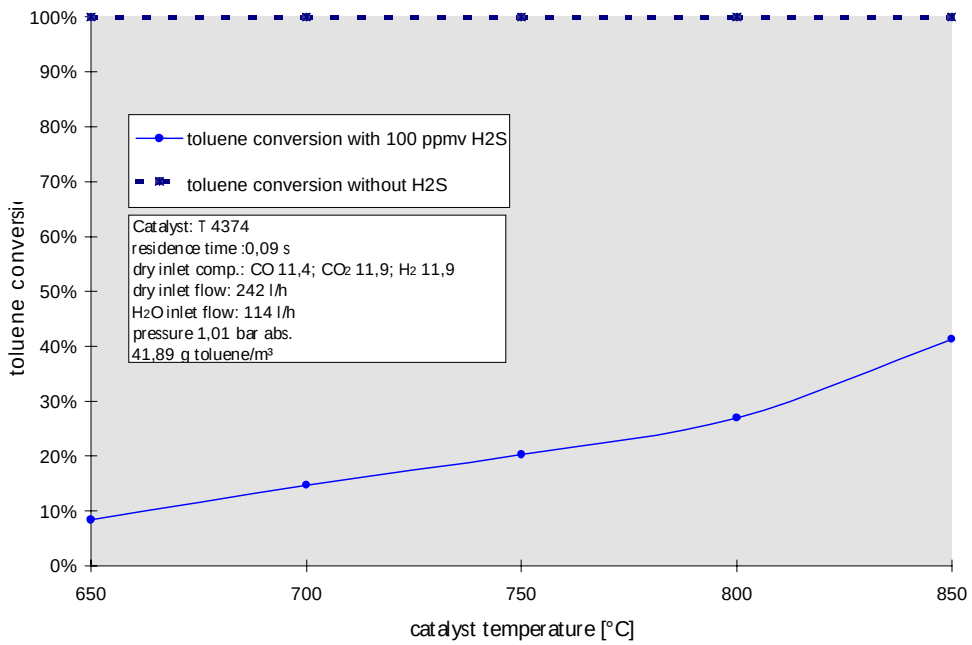

Figure 6: Comparison of toluene conversion in dependence on temperature in the catalyst bed with and without 100 ppm H_2S, catalyst T-4374

Though the catalyst T-4374 is known to be „sulfur resistant a temperature of 850°C is not sufficient for complete toluene conversion at presence of traces of hydrogen sulfide. The maximum conversion rate is about 40%. At higher temperatures a better conversion rate is expected, but was not experimentally realisable.

As summary, it can be stated, that pure organic model substances - benzene, naphtalene and toluene can be removed nearly completely by catalytic conversion at temperatures around 800°C. Impurities in the feed gas have an influence on catalyst activity and even sulfur resistant catalysts then require higher reaction temperatures. This temperature may even lie above the usual temperature of the gas at the exit of the gasifier, probably requiring an injection of air and thus a loss of hydrogen by combustion. Additionally, these idealized experimental conditions will not be comparable to real gasifier gases, containing a variety of organic compounds, sulfur and halogenes and probably even still containing dusts clogging the catalyst surface.

4.2. Sponge iron process

The **Sponge Iron Reaction (SIR)** process is a means of converting the energy of synthesis gases (e.g. derived from biomass gasification) to pure hydrogen applicable for electricity generation in a fuel cell. Thus it offers an alternative to the water gas shift reaction and subsequent fine purification[1,2]. The investigations aimed at assessing the SIR process in terms of feasibility, the subsequent practical realisation, optimisation of process variables and finally the simulation of the SIR process and its integration into a model of an entire electricity generation system in the range of 10 MW.

Principle

The SIR process is based on a redox reaction cycle of an iron ore contact mass which quasi serves as the „catalyst„. The process is operated in two conditions:

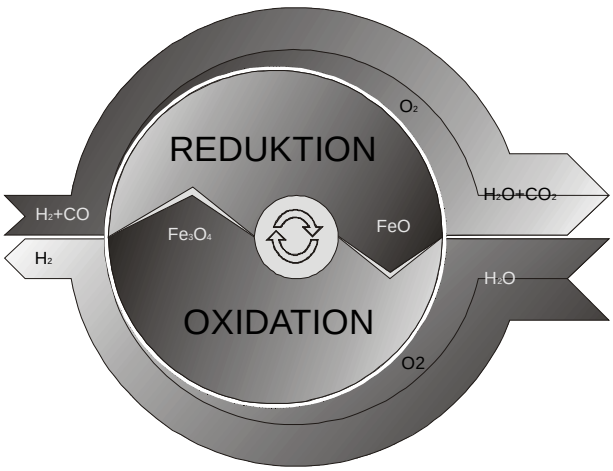

During the ***reduction step*** the iron ores are reduced by synthesis gas, whereby this gas is oxidised to a lean gas with low remaining CO and H_2 content. This lean gas is burnt. The thermal energy is further used for electricity generation or heat supply.

In the subsequent ***oxidation step***, the reduced iron ore is re-oxidised by water vapour which is thereby reduced to a hydrogen rich fuel gas composed of hydrogen and steam.

Figure 7: Principle of SIR

1 HACKER, V.; FUCHS, H.; FANKHAUSER, R.; SPREITZ, B.; FRIEDRICH, K.; FALESCHINI, G. (1998): „Hydrogen Production from gasified Biomass by Sponge Iron Reactor„, oral presentation and proceeding article, 12th World Hydrogen Energy Conference, Buenos Aires 21.-25.06.1998, Argentina

2 BARIN, I. (1992): „Thermochemical Data of Pure Substances„, Part I-II, VCH

In total the process converts CO and H_2 of synthesis gas to mere H_2. The two-steps principle of the process also represents the basis of the gas purification effect, as impurities that are either not bond during reduction or that are bond irreversibly to iron will not occur in the generated hydrogen.

Using gasified biomass, the redox reaction of iron ore takes only place between magnetite and wuestite. At a working temperature of 800°C, about 6% H_2 and 6-8% CO are retained in the lean gas, and water vapour during oxidation is converted to about 28% to H_2.

Selection of Iron Ore Contact Mass – The Pellet Concept

As contact mass, commercial iron ore pellets with a high porosity are employed. Pellets are produced from iron ore concentrates or powders in large scale (100t/h) by the iron and steel industry, whereby the pelletising process comprises the formation of so-called green pellets and after drying the firing (calcination) step. The fully reduced product is called sponge iron, from which the designation of the process is derived. The most vital requirements for applicability of a contact mass in the SIR are mechanical stability, low sintering tendency, high reactivity and constantly high conversion rates resulting in high cycle stability and thus long-term usage; finally it should be a low-price industrial bulk product.

Testing a variety of iron ore contact masses in a tube furnace device, SEK pellets (Voest Alpine, Linz) with the lowest iron content were best regarding mechanical and cycle stability.

After preliminary test of reaction behaviour over up to 20 redox cycles, pellet characterisation comprising the determination of inner surface area, electron microscopy of pellet fractures and determination of mechanical properties followed. Industrial and self-manufactured pellets were investigated in terms of pelletising process, structure stabilising agents and opportunities of improving conversion kinetics. For that purpose, commercial iron ore material was doped with foreign metals such as Co, Cu and Ni.

Process Investigation – Lab Scale SIR

For the theoretical investigation and for experimental set-up of the SIR process, a fixed bed reactor was chosen among various potential types. The self-constructed test stand consists of an electrically heated retort hanging on a balance, filled with up to 5 kg contact mass, connected to a gas supply (gas mixing station for simulation of biomass gas) and exhaust with gas analysis (figure 8). The process was studied under variation of the parameters temperature, amount of contact mass, gas composition, addition of „impurities„ (HCl, H_2S) and duration of reduction/oxidation. A standard gas composition is given in table 6. Long-term cycle stability over up to 36 redox cycles (48 hours) was tested out as well. The process was followed by on-line monitoring of weight and temperature as well as accompanying material and gas analysis. Generated hydrogen was determined volumetrically.

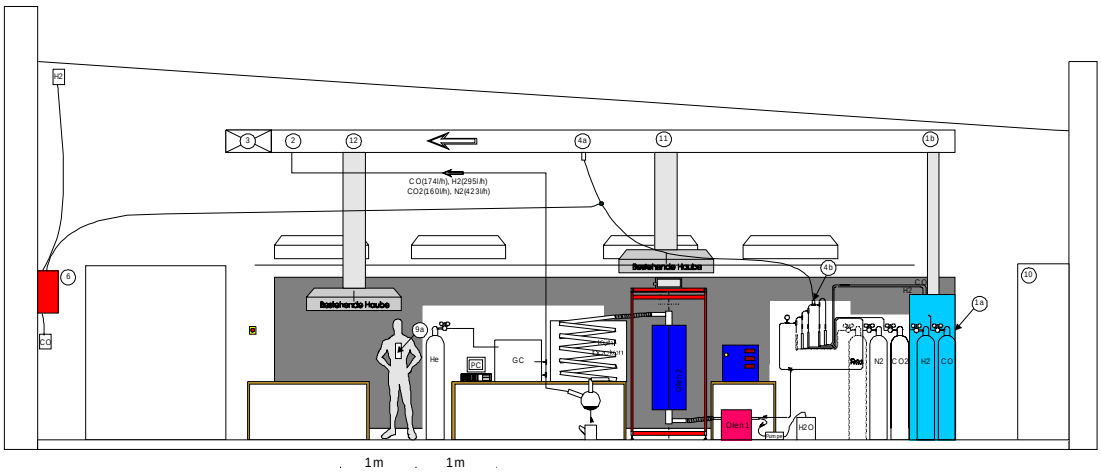

Figure 8: Test Stand of Lab Scale Sponge Iron Reactor

N_2	H_2	H_2O	CO	CO_2	HCl	H_2S
31-32	20-22	18-20	12-13	12-13	0 – 0,02	0 – 0,5

Table 6: Applied Standard Biomass Gas Composition (vol%), Total Gas Flow 1,052 m^3 at Ambient Temperature

Overview of Experimental Results

1. High working temperatures are favourable for a good hydrogen. Increasing temperature results in a better redox potential of biomass gas and oxidation, though not favoured thermodynamically, yields a similar H_2:H_2O ratio as with lower temperatures. High temperatures may, however, cause problems for the process as a whole, firstly what concerns mechanical equipment but also regarding its influence on total energy balance (in the awareness that higher gasification temperatures are only achieved under expediture of energy or oxygen addition).
2. Cycle stability of the used material was satisfactory up to 900°C. Cycle stability is a parameter to be optimised by process performance, the goal being an average life-time of the contact mass of 3 months at least. For an automated operation adherence to an optimum reactive zone is viable. The addition of H_2S as gas impurity had no influence on cycle stability
3. Considering biomass gas utilisation, we state that a good approximation to thermodynamic conversion is possible. Yet, efficiency is ideal only in the initial stages of reduction, then gradually declining until very low conversion rates in the vicinity of 100% wuestite and magnetite in case of oxidation, respectively. As reaction kinetics and biomass utilisation are only economic in a highly reactive zone in between, only the potential of about 40-50% is exploited for practical purpose.

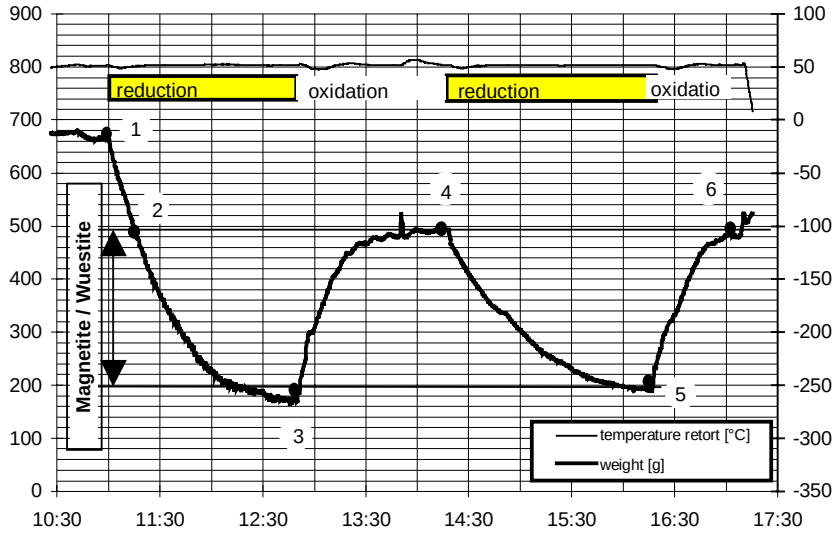

Figure 9: Redox Reactions to Equilibria followed by Balance, Load 3,5 kg SEK Pellets, 800°C

4. Consequently, hydrogen productivity (itemised to mass of iron ore material) is best in a narrow reactive zone. Hydrogen production per kg of pellet material per hour (measured over 5 total cycles) in dependence of temperature and percentage of conversion (theoretical magnetite-wuestite conversion) is depicted in table 7.

Temperature [°C]	800		900
Reactive zone: % of total conversion	49,7	42,3	49,2
H_2-Productivity [NL per kg material/h]	15,8	22,8	28,2

Table 7: Hydrogen Production [Norm Litres /kg.h]

So, the total redox field of the contact mass between magnetite and wuestite cannot be exploited, what results in a higher requirement of total pellet mass. The hydrogen storage capacity of SEK-wuestite is 67 Nm^3 hydrogen per 1000 kg.

5. The level of purity of generated hydrogen from CO necessary for application in any fuel cell could be achieved. H_2S is apparently bond to Fe in the sponge iron and does not pollute the product gas stream. HCl is not retained by the iron permanently, the bulk going through without reaction and is recovered in the lean gas. Parts of HCl are found in the oxidation gas stream, but can be removed from hydrogen by water condensation. The very long-term influence of these impurities (especially H_2S) on SIR operation and accumulation effects in the contact mass are difficult to predict.

Design of a Demonstration Plant

On the basis of thermodynamic[3,4] and kinetic data[5] from literature as well as experimentally derived kinetic data, a simulation of the SIR as integrated part of electricity generation was carried out.

Parameters for Calculation and System Concept

The heating capacity of the applied biomass equals 10MW and is calculated by the Lower Heating Value. This biomass is pre-dried in a dryer and converted in a gasifier to synthesis gas which is afterwards fed in the Sponge Iron reactor to produce hydrogen. The average working temperature is 800°C.
For simulation the software IPSEpro was used.

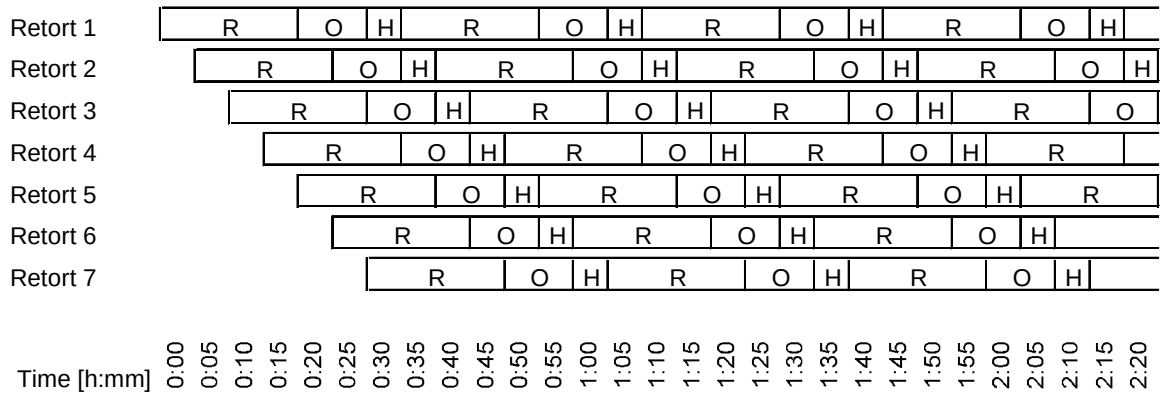

Figure 10: Timetable of Process Steps in the Retorts

From data of the lab scale reactor the number of retorts was calculated as follows

- Four retorts for the reduction
- two retorts for the oxidation and
- one retort for the intermediate heating step are applied at the same time.

The seven retorts are connected in parallel. A further retort is required to enable the pellet exchange during working time.

The amount of the contact mass used depends primarily on the synthesis gas, which should be converted to hydrogen as complete as possible. About 45 tons of sponge iron material are needed to process the synthesis gas from the gasifier (calculated production 18000 m^3/h at 800°C). That results in a dimensioning of the complete apparatus of about 6,5 meters in length, 6,5 meters in width and 6 meters in height.

---

3 BOGDANDY, L. v.; ENGELL H. J. (1967): „Die Reduktion der Eisenerze„, Wissenschaftliche Grundlagen und technische Durchführung, Düsseldorf

4 HÖRSGEN B. (1979): „Zur Berechnung des Stoff- und Wärmeaustausches im Lurgi-Druckreaktor„, Dissertation, RWTH-Aachen

5 HACKER, V.; FALESCHINI, G., FUCHS, H.; FANKHAUSER, R.; SIMADER, G.; GHAEMI, M.; SPREITZ, B.; FRIEDRICH, K. (1998) Usage of biomass gas for fuel cells by the SIR process, Journal of Power Sources 71, 226-230

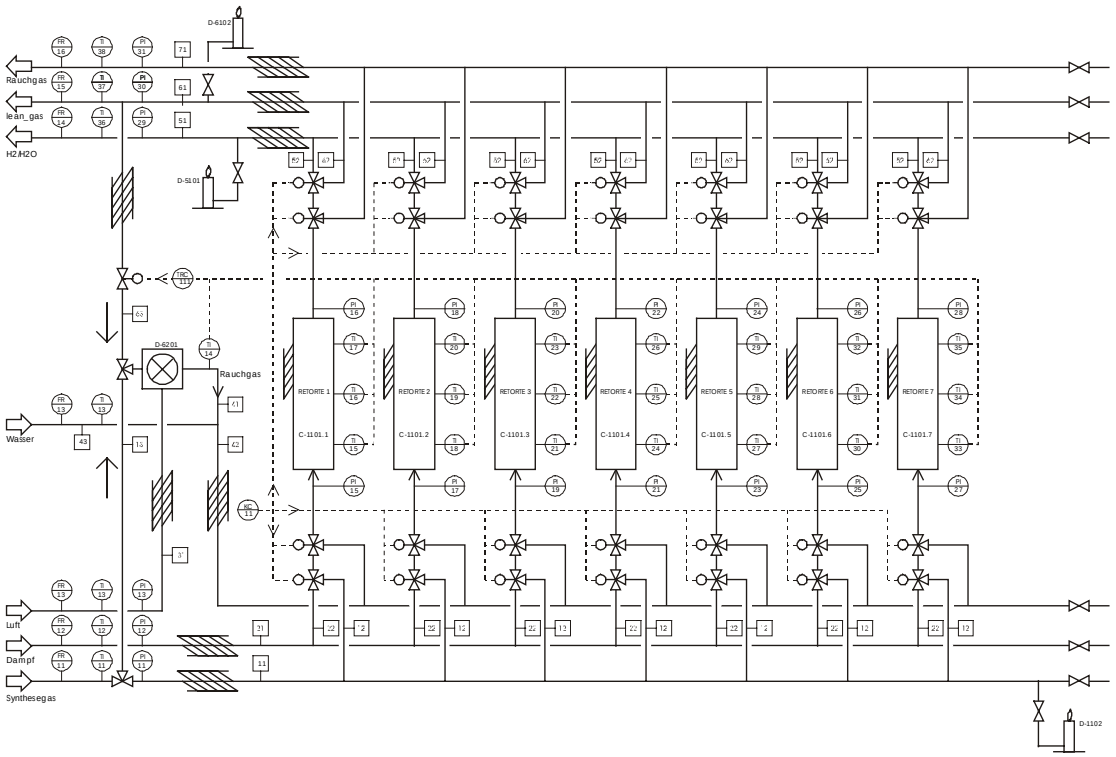

Figure 11: Connection Diagram of Sponge Iron Reactor

An efficiency of 50% for the SIR alone related to the input of synthesis gas was calculated. The efficiency of electricity generation of the process chain biomass dryer-biomass gasifier-SIR-SOFC is calculated to 25%. An overall efficiency comprising electricity as well as utilisable heat can be estimated to 35%.

4.3. CO-shift

The shift conversion reaction converts carbon monoxide to hydrogen

$CO + H_2O \rightarrow CO_2 + H_2$

The thermodynamical equilibrium of these reaction depends on temperature and on the steam content of the gas. According to the gas composition given in the gasifier outlet, the steam to carbon ratio (S/C) is 0,77 for gasified wood. With this relatively low steam content, a concentration of 0,5 % of CO is remaining in the gas at the lower limit of the operation temperature of shift reactors. Quenching with liquid water is one possibility to increase the steam content and to cool the gasifier gas down to the operation temperature of the shift converters. For industrial hydrogen production processes, usually a two or even three staged process is chosen. Therefore, different catalysts for different ranges of operation temperature are commercially available. The data of the catalysts used are given in table 8.

reaction	abbreviation	catalyst	active component
high temperature shift	HTS	G3-C, Südchemie	Fe, Cr
low temperature shift	LTS	G-66A, C18-7, Südchemie	Cu, Zn

Table 8: Composition of shift conversion catalysts

Under isothermal conditions and at low gas velocity thermodynamic equilibrium is always achieved. But in real reactors, usually isothermal conditions are not realised due to the reaction heat. Thus an integral reactor with a heat exchanger was designed for both reactions, HTS and LTS. The measurements were carried out with a typical gasifier gas after dust and tar removal.

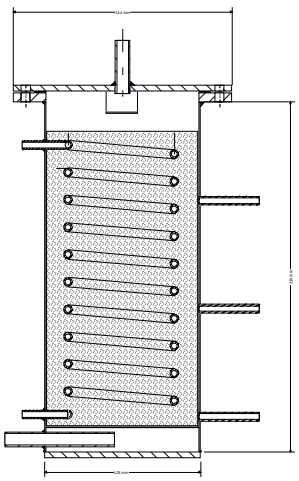

Figure 12: Test shift reactor design

The effect of the gas hourly space velocity (GHSV) on the CO conversion in both shift reactors was investigated with the gas mixture

N_2	35 Vol-%
H_2O	20 Vol-%
H_2	17 Vol-%
CO und CO_2	12 Vol-%
CH_4	4 Vol-%

The GHSV was varied between 667 and 2500 h^{-1}. For this gas composition, the steam-to-total gas ratio is 0,25, this is significantly below the value recommended by the catalyst manufacturer (0.4) so that a deposition of carbon could not principally be excluded.

The product gas was separately analysed after the high temperature converter and after the low temperature converter. The results of the six runs are given in Figure 13 in terms of CO-content in the exit gas of the LTS. For higher space velocities, approximately above 1700 h^{-1}, the experimentally determined CO content tended to exceed the thermodynamic values. This indicates either a kinetic limitation or a somewhat higher average operation temperature compared to the measured values.

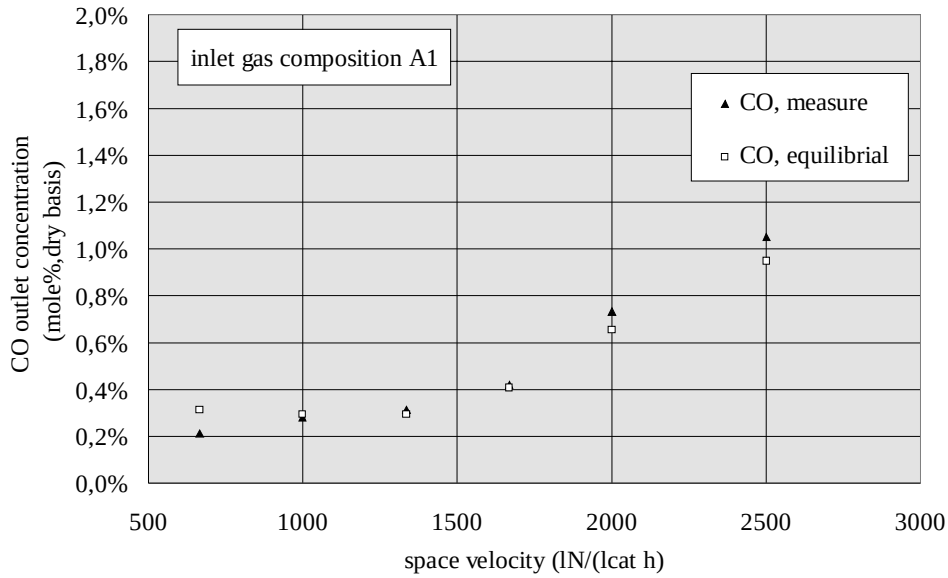

Figure 13: CO-content of the shift gas as function of space velocity

The temperatures in the low temperature shift reactor were relatively low at low space velocities, at higher flows, a considerable temperature increase at the reactor inlet is observed. The reason is the increased CO content at the reactor inlet, because the CO-conversion in the high temperature shift was more and more incomplete. A feasible space velocity for the shift is in the range 1000 - 1500 h^{-1}. Higher values may be possible under optimised thermal conditions.

4.4. Fine Purification

The work of the University of Duisburg is focused on a very high gas purity and an extremely low carbon monoxide content to provide hydrogen for a PEM fuel cell. The selected gas purification system has on the one hand to work with respect to the gasified biomass, the gas composition and the possible impurities of the feed gas and on the other hand due to the demands of the selected fuel cell.

Generally the following commercial gas purification systems can be distinguished:

- sulphur removal with adsorbents or in accordance with chemical reactions
- carbon monoxide conversion by the watergas reaction (shift reaction)
- selective carbon monoxide methanation
- selective oxidation of carbon monoxide (PROX)
- pressure swing adsorption (PSA)
- gas absorption with subsequent methanation
- metal membrane diffussion
- iron sponge purification

A carbon monoxide management system is required to lower the CO concentration with a CO content of 0.5 to 1 % behind the shift conversion steps to acceptable levels of 5 to 20 ppmv for a PEMFC. In many cases the CO reduction system consists of a combination of several of the above processes to achieve the necessary reduction in CO content. So the two fine purification processes using a palladium membrane and a

carbon dioxide scrubber with subsequent methanizer are main points of the theoretical and experimental investigations. The experiments of the gas liquid scrubbing system are carried out with polymer membranes, which is a newly and innovative technology specially for small applications. The tested palladium membrane is a commercial available product with an extremely thin metal lattice.

Results of carbon dioxide scrubbing

The established technology for removing carbon dioxide of gas streams is amine absorption. Generally conventional equipment such as packed columns or tray columns are used as gas-liquid-contactors. Membrane gas absorption is a new method for gas separation which makes use of membranes for the transfer of components between the gaseous phase and the liquid. The membrane forms a permeable barrier and components like CO_2 diffuse through the membrane and are absorbed by the liquid. Membrane contactors have operational and economical benefits over conventional equipment. The use of a membrane in the form of low cost hollow fibres (e.g. polypropylene) enlarges the contact surface area of more than 500 m^2/m^3 between the gas and the liquid phase, which is independent of the gas and the liquid flow rates.

In contrast to membrane separation technologies, where the permeability coefficient is mainly influenced by the membrane material, the choice and the concentration of the absorption liquid has to be considered additionally for scrubbing processes. Different absorption liquids are used for the absorption of carbon dioxide, by name monoethanolamine (MEA) and methyldiethanolamine (MDEA) have been tested in the experimental setup. So it is useful to fix the permeability coefficient P_i for the whole system, membrane and absorption liquid. In table 9 the coefficients given by the experimental results are shown.

Membrane-module	***Absorption liquid***	***Permeability coefficient P_i***
PP-fibres (Type 1)	5 mole-% MEA	32.25 l/(m² min bar)
PP-fibres (Alternative module)	5 / 10 mole-% MEA	0.115 l/(m² min bar)
	5 mole-% MDEA	0.063 l/(m² min bar)
PTFE-membrane sheet	5 mole-% MEA	17.5 l/(m² min bar)
PDMS-fibres	5 mole-% MEA	2.9 l/(m² min bar)

Table 9: Experimental results for permeability coefficients

Although the permeability coefficient of the system membrane type 1 with 5 mole-% mono-ethanolamine is nearly 32.25 l/(m² min bar), it must be recognized, that no chemical longterm stability is given. On the other hand the PP-fibres of the alternative membrane module constitutes a stable system with amines like MEA or MDEA. During the experimental period of 6 weeks no decomposition effects could be observed, but it must also be mentioned that the permeability coefficient of 0.0625 to 0.115 l/(m² min bar) is clearly lower than for the other system. For the non-porous membrane with the PDMS top layer the permeability coefficient is nearly 2.9 l/(m² min bar). The system is not a stable one and unsuitable for the absorption of carbon dioxide with amines. The permeability coefficient of the porous PTFE-module is in the range of 17.5 l/(m² min bar) and on the scale of the PP-module type 1. The great advantage of this material is the chemical longterm stability, necessary for the absorption process.

Although the PTFE-membrane sheet is expensive, it shows an excellent behaviour for the absorption of carbon dioxide. With respect to the high permeability coefficient and to chemical longterm stability the PTFE-membrane is suitable for the considered scrubbing process step. With the experimental results it is possible to design the volume and the purification degree of a scrubbing system with longterm stability.

Results of hydrogen separation with palladium-silver membranes

For the experimental investigations a palladium alloy membrane is used with a silver rate of 23 wt.-%. The membrane is a product of Johnson Matthey Noble Metals, Royston UK, with a membrane thickness of 7.5 mm and a membrane surface of 140 cm^2. The metal membrane is placed in a tubular membrane chamber. The influence of discrete gases to the hydrogen permeation through a palladium membrane was investigated in a series of experiments. The gas composition had been chosen according to the cases of application of a palladium membrane for the purification of hydrogen gases. Permeation measurements through the JMM-membrane module have been carried out for different polynary gas mixtures with different volume proportions of hydrogen, carbon monoxide, carbon dioxide, nitrogen, methane and water vapour at temperatures of 310 °C and 450 °C. The permeation rates determined for the gas mixtures composed according to Noell-data are shown separately in Figure 14 for a membrane temperature of 310 °C and in figure 15 for 450 °C.

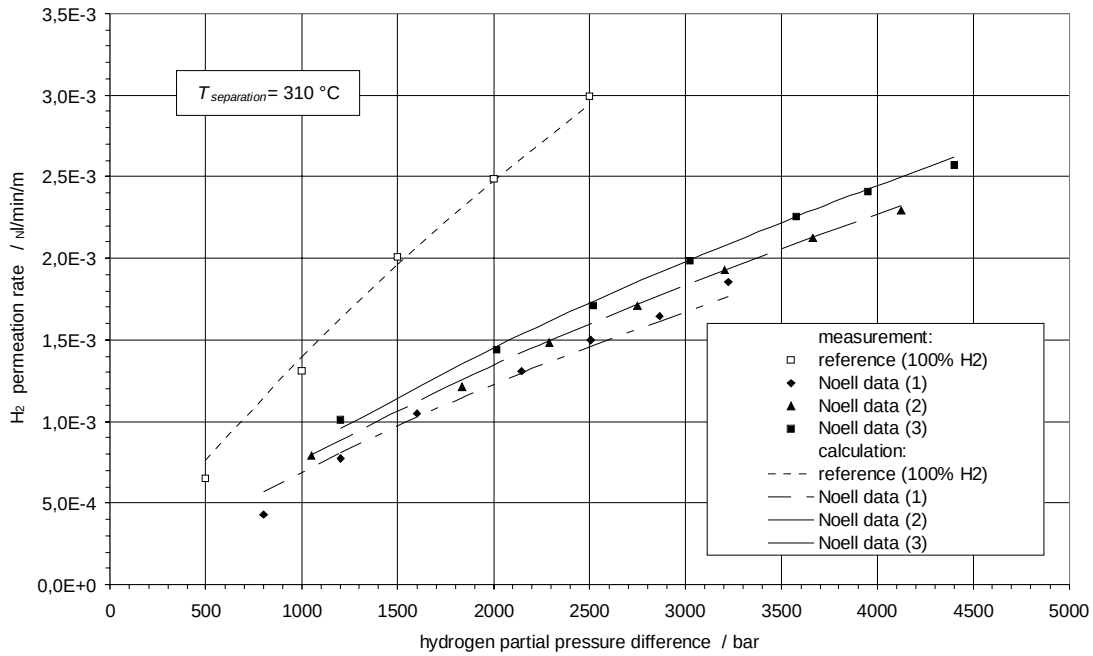

Figure 14: H_2-permeation rates of the Noell gas mixtures at 310 °C

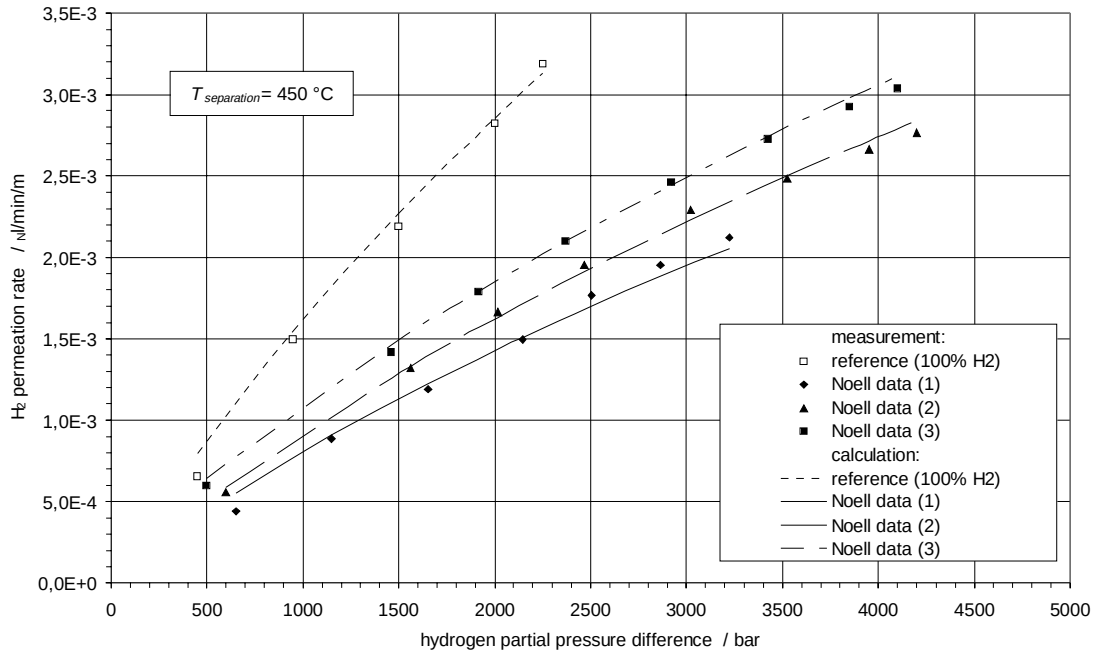

Figure 15: H_2-permeation rates of the Noell gas mixtures at 450 °C

A further evaluation parameter of the gas separation is the production factor R_i and, for the given case of hydrogen separation, R_{H2}, respectively. It describes the interrelationship between the mole flow of the hydrogen in the pure gas (indexed *P*) and that in the feedgas (indexed *F*):

$$R_{H_2} = \frac{N_{H_2,P}}{N_{H_2,F}}$$

Figures 14 and 15 show the hydrogen separation production rates determined at 310 °C and 450 °C for the feedgas mixture composed according to Noell-data. At increasing hydrogen partial pressure difference between feedgas side and pure gas side, the permeation rate and consequently the production rate R_{H2} increases.

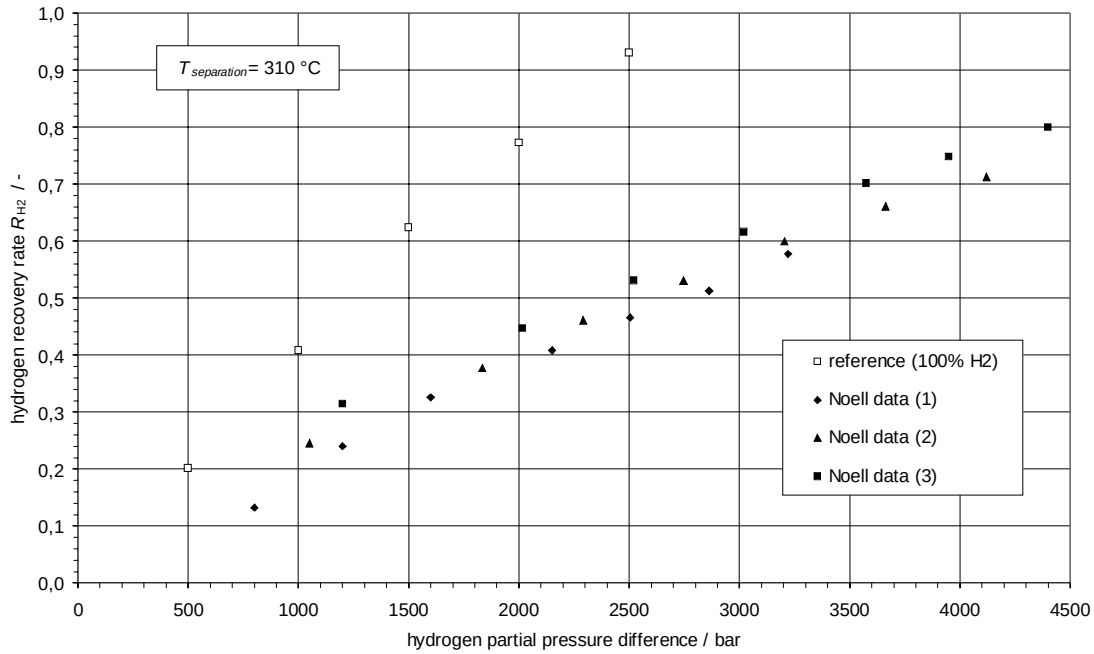

Figure 16: Production rates R_{H2} of the H_2-separation at 310 °C according to Noell-data

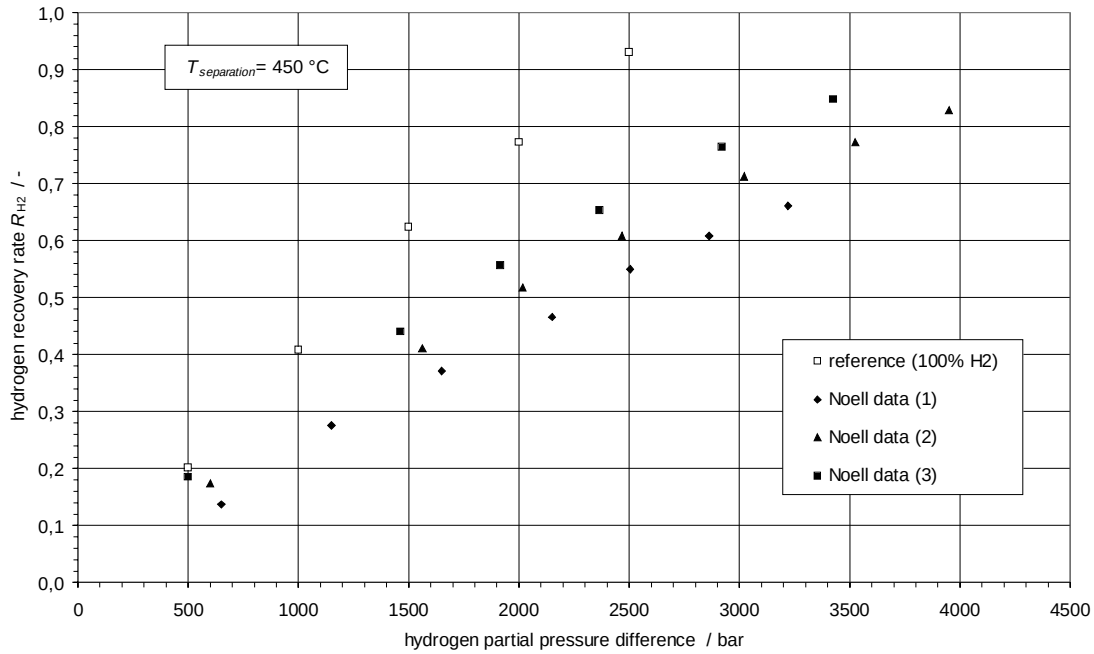

Figure 17: Production rates R_{H2} of the H_2-separation at 450 °C according to Noell-data

4.5. Fuel cell demands

The conversion of gasified biomass into electrical energy is possible by various electricity generators:

- gas turbines
- diesel, Otto or Stirling engines
- the various types of fuel cell

Each of these generators has different requirements with respect to the gas purity and each generator causes typical emissions. The choice of a suitable generator for a special application mainly depends on the required power. Gas turbines are available in the MW-power range and show good efficiency during continuous operation at full load. Technical adaptation to the woodgas is necessary due to its quite low heating value. The engines are much more flexible with respect to load and are available from a power of 30 kW upwards. The Stirling engine is a special case, as there is no commercial production of these type of engine up to know. The combustors and heat exchangers of Stirling engines must be specially adapted to gasified biomass[6]. The fuel cells up to now have a quite different state of development and will be described in the following sections. Fuel cells show good conversion efficiencies even in the low power range, during the electrochemical conversion process of the fuel, the power generating process, no additional emissions are generated.

The types of fuel cells

The different types of fuel cells are usually classified according to the electrolyte used. The electrolytes can be solid or liquid and show best conductivity at different temperatures and humidity conditions. The types of fuel cells are listed in table 9. For each fuel cell, a chapter with the most important data is given: The main criteria for selection of a fuel cell are

- Technical: the required gas purity of the fuels, operation conditions and efficiency
- Economical: availability and cost

6 E. Münster, "40 kW Stirling engine powered by wood chips", Biomass for energy and environment 2, 1280 (1996)
J. M. Martinez, R. Escalada, J.M. Murillo, L.S.Esteban, J.E.Carrasco, "Development of a congeneration plant by combustion of biomass in an AFB combustor and heat conversion into electricity a Stirling engine V-160" Biomass for energy and environment 2, 1239 (1996)

Fuel cell system	electrolyte	tempe-rature (°C)	efficiency (%, LHV of dry fuel)	fuel	applications	degree of commer-cialisation
AFC alkaline fuel cell	30% KOH	80	40-60	pure hydrogen, for methane, external reforming and gas purification required, even CO_2 sensitive	space missions, military	--
PEMFC polymer electrolyte membrane fuel cell	solid polymer membrane	80	50-60	hydrogen, else exter-nal reforming, gas purification required, very CO sensitive, CO_2 insensitive	electric traction, military, space missions	+
PAFC phosphoric acid fuel cell	conc. phosphoric acid	200	40 - 50	hydrogen, else exter-nal reforming, CO sensitive, CO_2 in-sensitive	cogeneration units (heat:180°C)	++
MCFC molten carbonate fuel cell	eutectic mix-ture of Li and K carbonate	650	50-60	natural gas, internal or external reforming possible	cogeneration units, power plants	+
SOFC solid oxide fuel cell	ceramic solid electrolyte: yttrium stabi-lised zirconium oxide	900-1000	50-60	hydrogen or natural gas	cogeneration units, power plants	-

Table 10: The types of fuel cells listed in the order of increasing operation temperature

The components to be removed prior to feeding the gas to the different fuel cells are for all types dust exceeding a certain particle size and condensing tars. The requirements - as far as available in literature - of the five types of fuel cells are depicted in figure 18 and summarised in table 11.

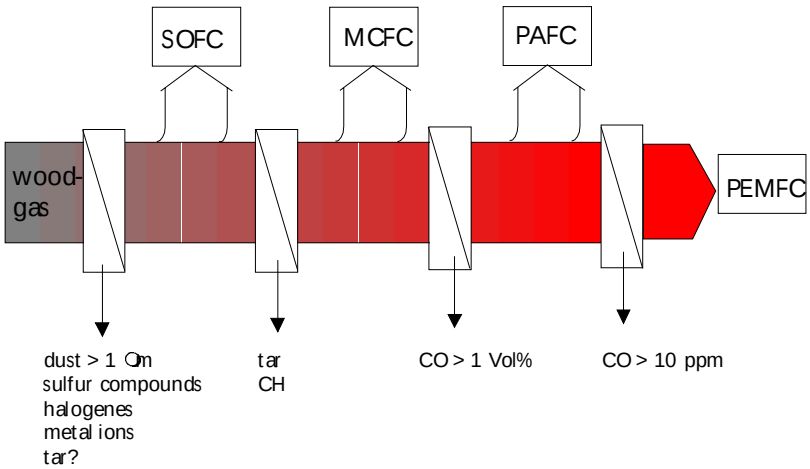

Figure 18: Impurities to be removed prior to feeding the gas from wood gasification to fuel cells

type of fuel cell operation T	dust	tar	other impurities to be removed	CO-content
SOFC 1000 °C	not investigated, but probably similar as MCFC	toluene causes no problems, no tar condensation due to high operation T	H_2S causes a reversible performance loss	is a fuel
MCFC 650°C	< 1 micron in size	CH < 1 Vol-% condensing tars must be removed	sulphur, halogenes, lead	is a fuel
PAFC 200 °C	not investigated, but very low	not investigated, will condense	H_2S, COS NH_3	< 0,5 Vol-%
PEMFC	not investigated, but very low	not investigated, will condense	HCOOH	< 30 ppm

Table 11: Literature data on required fuel purity

4.6. Plant simulation and cost estimation

Simulation for the different types of gas cleaning have been performed by TU Graz und UNI Duisburg. The Technical University of Graz has used the software IPSEPRO (company SimTech) whereas Uni Duisburg has used ASPEN.

Both universities have simulated the whole process also including the steps drying, air preheating, gasification and fuel cell and individually for their gas cleaning steps (TU Graz have performed a simulation of the SIR and Uni Duisburg did the same for membrane and absorption process).

Therefore, it was important to fix the starting conditions for the simulation (e.g. biomass composition). The biomass composition used for the simulation was the following one:

	biomass input (waf)	mole-stream	mass-stream
C	51,09 weight-%	90,963 kmol/h	1092,56 kg/h
H	5,46 weight-%	57,908 kmol/h	116,735 kg/h
N	0,203 weight-%	0,155 kmol/h	4,341 kg/h
O	43,22 weight-%	28,884 kmol/h	924,260 kg/h
H_2O_{liquid} (w=30 %)	water free	50,873 kmol/h	916,5 kg/h
S	0,022 weight-%	0,015 kmol/h	0,047 kg/h
Cl	0,013 weight-%	negligible	negligible
Dry biomass	H_U = 17,949 MJ/kg	177,9 kmol/h	2138,5 kg/h
Moist biomass	H_U = 11,785 MJ/kg	228,8 kmol/h	3055 kg/h

Table 12: Biomass composition

For the first step 4 different variants have been simultated to show the influence of moisture content and of air preheating.

Case I: Moist biomass (w=30 %) without drying and without air preheating

Case II: Moist biomass (w=30 %) without drying and with air preheating

Case III: Biomass with 50% drying (w=17,65 %) and without air preheating

Case IV: Biomass with 50% drying (w=17,65 %) and with air preheating

The base for the simulation was that all of the following equations and equilibria should be fullfilled. Especially in the case of the equlilibrium of the methane formation the amount of methane was fixed to 4 % in accordance to experimental results obtained by NOELL.

Equations and Equilibria

- the partial combusting ($C + 0{,}5\ O_2 \leftrightarrow CO$),
- the total combustion ($C + O_2 \leftrightarrow CO_2$),
- the *Boudouard* reaction ($C + CO_2 \leftrightarrow 2\ CO$),
- the heterogenous water gas reaction ($C + steam \leftrightarrow CO + H_2$),
- the methane formation ($C + 2\ H_2 \leftrightarrow CH_4$; $CO + 3\ H_2 \leftrightarrow CH_4 + H_2O$),
- the homogeneous water gas reaction ($CO + steam \leftrightarrow CO_2 + H_2$).

The two different software packages have different approaches to solve this system of equations. IPSEPRO solves the equation numerically without using further data and ASPEN calcutes the Gibbs energy and minimizes it. The results obtained were very similar, but little differences appeared. . The following table shows the results of Uni Duisburg for the gas composition of the gasifier gas.

		Case I	Case II	Case III	Case IV
		Moist biomass No air preheating	**Moist biomass Air preheating**	**dry biomass no air preheating**	**dry biomass air preheating**
Total volume flow	[m^3/h]	27557,4	23375,6	26735,4	22831,9
Total mass flow	[kg/h]	7934,9	7489,8	7572,9	7154,9
Total mole flow	[kmol/h]	308,996	297,809	299,780	289,102
Pressure	[bar]	1	1	1	1
Temperature	[°C]	800	800	800	800
Gasifying air	[m^3/h]	4193,5	3811,1	3882,5	3523,3
λ-value	[ ]	0,3886	0,3532	0,3598	0,3265
H_2	[%]	**10,6**	**12,5**	**12,1**	**14,0**
	[kmol/h]	32,787	37,304	36,330	40,382
N_2	[%]	**43,4**	**40,9**	**41,4**	**38,9**
	[kmol/h]	133,942	121,742	124,014	112,558
CO	[%]	**9,4**	**11,1**	**10,8**	**12,4**
	[kmol/h]	29,121	33,081	32,244	35,817
CO_2	[%]	**16,0**	**15,5**	**15,6**	**15,1**
	[kmol/h]	49,497	46,043	46,728	43,546
CH_4	[%]	**4,0**	**4,0**	**4,0**	**4,0**
	[kmol/h]	12,345	11,839	11,91	11,600
H_2O	[%]	**16,6**	**16,0**	**16,2**	**15,6**
	[kmol/h]	51,289	47,784	48,455	45,185

Table 13: Gas composition downstream the gasifier for the different biomass treating cases

After the gasification step the gas cleaning steps were different, so no comparison can be made for the additional steps.

In the case of the SIR process the gas deriving from the gasifier is led to the SIR reactor without any further cleaning. In the first step the gas reduces the iron sponge and the gas leaving the reactor (lean gas) is burned to form heat and power. In the next step steam is led into the reactor to oxidise the reduced iron sponge and thus producing pure hydrogen. The hydrogen is then used in the fuel cell. The off-gas preheates the air for the fuel cell.

The following flowchart shows on the modifications of the process.

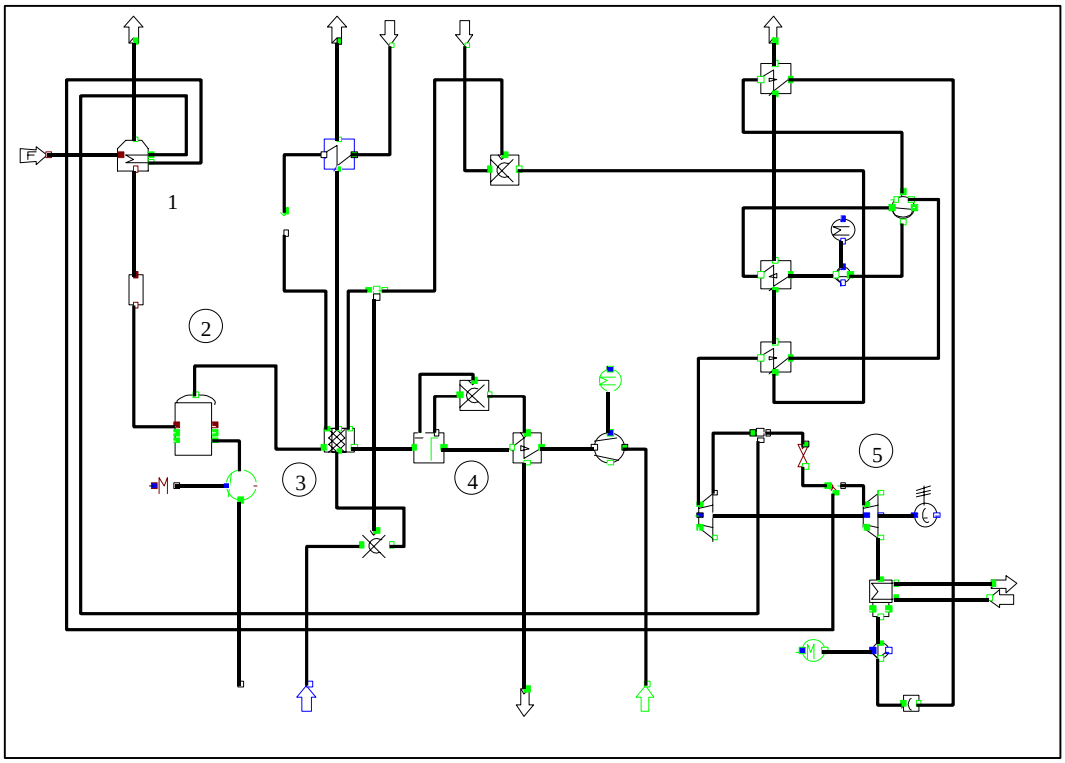

Figure 19: Flowchart

The following table shows the electric outputs and the total efficiencies for all modifications of the whole process.

			Electricity [kW]			
Case	Drying	Air preheating	Fuel cell	Steam turbine	Energy consumption	Efficiency [%]
1			1997	756	301	24,5
2	X		2158	716	381	24,9
3		X	2430	365	336	24,6
4	X	X	2572	331	408	25,0

Table 14: Electric output and efficiency

The implementation of the shift conversion reactors requires additional devices. Behind the wood gasifier and the air preheater the water nozzle follows (figure 20), in order to reach the steam to carbon ratio S/C of 3 for the shift reaction. A higher steam to carbon rate would increase the hydrogen mole-flow and even the carbon monoxide content would be decreased. Because of the water nozzling the gas stream is cooled down, for a steam to carbon ratio of 4 below the shift reaction temperature and so an additional preheating would be necessary. To avoid the preheating the fixed value of S/C=3 is valid for the following calculations. All results of the shift simulation are shown in table 15.

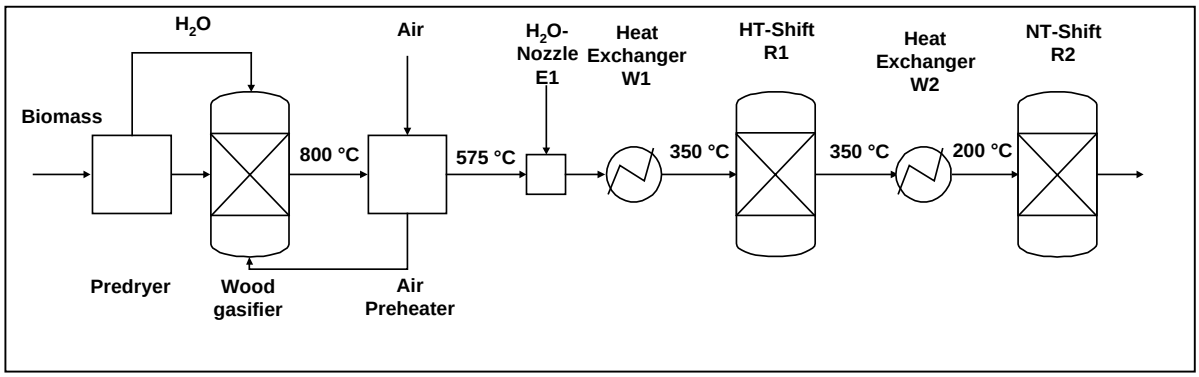

Figure 20: Flowsheet of gasifier and shift steps

	Case I	Case II	Case III	Case IV
	moist biomass no air preheating	**moist biomass air preheating**	**dry biomass no air preheating**	**dry biomass air preheating**
Total volume flow[m^3/h]	14546,1	14671,4	14635,7	14735,2
Total mass flow [kg/h]	8584,7	8416,9	8442,6	8276,6
Total mole flow [kmol/h]	369,760	372,945	372,039	374,568
Pressure [bar]	1	1	1	1
Temperature [°C]	200	200	200	200
Water injection [kmol/h]	36,074	51,459	48,277	62,266
S/C [ ]	3	3	3	3
H_2 [%]	**29,8**	**31,3**	**31,0**	**32,5**
[kmol/h]	110,089	116,723	115,484	121,663
N_2 [%]	**36,2**	**32,6**	**33,3**	**30,1**
[kmol/h]	133,942	121,742	124,014	112,558
CO [%]	**0,3**	**0,3**	**0,3**	**0,2**
[kmol/h]	1,199	1,018	1,054	0,936
CO_2 [%]	**24,3**	**24,1**	**24,2**	**24,0**
[kmol/h]	89,764	89,945	89,910	90,028
CH_4 [%]	**traces**	**traces**	**traces**	**traces**
[kmol/h]				
H_2O [%]	**9,4**	**11,7**	**11,2**	**13,2**
[kmol/h]	34,751	43,502	41,559	49,369

Table 15: Results of the main gas characteristics after shift reaction

Simulation of the scrubbing process

The biomass gas leaving the shift stages with the composition presented in table 16 enters the fine purification system. First the carbon dioxide scrubber with subsequent methanizer, then the palladium-silver membrane is the main point of interest for the simulations. The simulation

flowsheet of the carbon dioxide absorption process is shown in figure 21. If a suitable absorbent is chosen, the carbon dioxide is selectively and totally removed in the absorber. For the carbon dioxide removal alkanolamines like monoethanolamine (MEA) or methyldiethanolamine (MDEA) are mostly used in industrial applications. The absorbent choice for the simulation is 10 mole-% MEA in water, resulting from an extensive study of the *Absorber* simulation model with electrolyte reactions. A lower mole concentration causes a higher energy demand for the desorption because of the additional water content, which has to be heated up. A higher MEA concentration has the disadvantage of lower corrosion-resistant. As result of the energetic optimisation for 10 mole-% MEA the optimal mole-proportion for the amine purification process amounts approximately 4 moles amine per mole carbon dioxide. In the table 17 the simulation results for the different gasification cases are presented. The total efficiency is listed in dependence on the case of gasification in table 18.

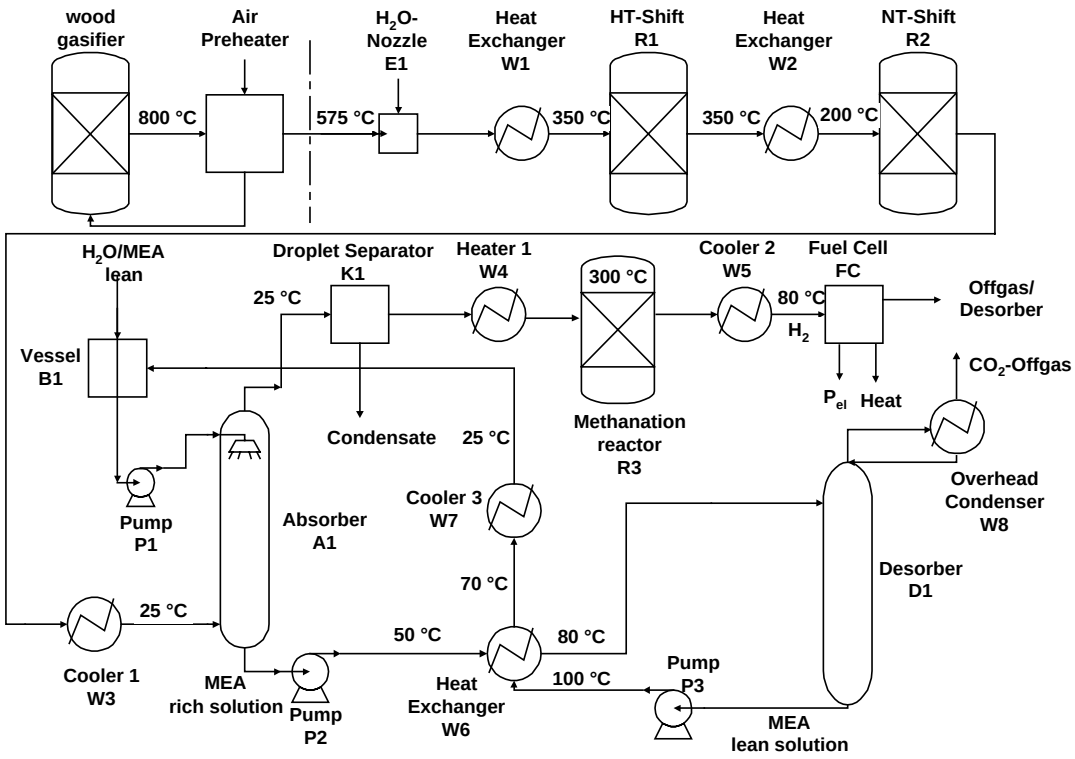

Figure 21: Flowsheet for carbon dioxide scrubbing with subsequent methanation

		Case I	Case II	Case III	Case IV
		moist biomass no air preheating	**moist biomass air preheating**	**dry biomass no air preheating**	**dry biomass air preheating**
Total volume flow	[m^3/h]	7651,9	7493,9	7523,0	7362,6
Total mass flow	[kg/h]	4339,9	4007,8	4069,6	3752,6
Total mole flow	[kmol/h]	260,592	255,202	256,195	250,725
Pressure	[bar]	1	1	1	1
Temperature	[°C]	80	80	80	80
H_2	[%]	**41,8**	**45,3**	**44,6**	**48,1**
before Methanation	[kmol/h]	110,089	116,723	115,484	121,663
H_2	[%]	**40,6**	**44,2**	**43,5**	**47,1**
behind Methanation	[kmol/h]	105,705	112,785	111,458	117,968
N_2	[%]	**51,4**	**47,7**	**48,4**	**44,8**
	[kmol/h]	133,946	121,745	124,020	112,561
CO	[%]	**0,5**	**0,4**	**0,4**	**0,4**
before Methanation	[kmol/h]	1,199	1,017	1,054	0,935
CO	[%]	***traces***	***traces***	***traces***	***traces***
behind Methanation	[kmol/h]				
CO_2	[%]	***traces***	***traces***	***traces***	***traces***
	[kmol/h]				
CH_4	[%]	**0,5**	**0,5**	**0,5**	**0,5**
	[kmol/h]	1,407	1,249	1,281	1,168
H_2O	[%]	**7,5**	**7,6**	**7,6**	**7,6**
	[kmol/h]	19,534	19,423	19,436	19,028

Table 17: Gas characteristics after carbon dioxide scrubbing and methanation

	Case I	Case II	Case III	Case IV
	moist biomass no air preheating	**moist biomass air preheating**	**dry biomass no air preheating**	**dry biomass air preheating**
Total Efficiency Gasification η_V [%]	73,95	78,41	77,57	81,72
Total Efficiency Absorption η_{AII} [%]	98,99	89,03	96,61	87,92
Total Efficiency Methanation η_M [%]	96,01	96,62	96,52	96,97
Total Efficiency Gasification and Gas Purification η_G [%]	***70,28***	***67,45***	***72,33***	***69,67***
Efficiency of Fuel Cell η_{FC} [%]	***37,50***	***37,50***	***37,50***	***37,50***
Total Efficiency η_{gesW} [%] ***complete Process***	***26,36***	***25,30***	***27,12***	***26,13***
Electric performance P_{elW} [MW] ***complete Process***	***2,636***	***2,530***	***2,712***	***2,613***

Table 18: Efficiencies for the absorption process with subsequent methanation

The total efficiency is the product of the separate efficiencies. Because of the fact that a hydrogen mixture with less than 50 % hydrogen is fed into the fuel cell, the fuel cell efficiency is set to 37,5 %. The offgas, which contains 25 % of the hydrogen input, is internally used for desorber heating and is taken into consideration for the absorption process. The combination of gasfication and absorption efficiency is characteristic for an evaluation of the total process because of internal heat use. In the case of no air preheating the sensible heat of the biomass gas is used for the desorption process and so the absorption efficiency is increased. In the case of preheating and drying of biomass the gasification efficiency is maximal, but the remaining desorption energy can not be taken away from the sensible heat and has additionally to be generated by the combustion of a part of the biomass gas. The efficiency of the gasification plus gas purification lies between 67,5 and 72,5 %. The efficiency for the complete process, including electricity generation in the fuel cell, amounts 25 to nearly 27 %. That means an electric performance of 2,5 to 2,7 MW could be produced, if a biomass input of 10 MW is given. The highest electric output is given for the case of biomass drying. The air preheating shows insignificant lower performance after heat integration, but in comparison to the simulation results it is customary for real gasification plants because of non-ideal behaviour. Beside the electricity generation a heat stream of equal amount (2,5 to 2,7 MW) is leaving the fuel cell at a temperature of 80 °C in the condition of water

Simulation of the palladium-silver membrane

The simulation flowsheet for the hydrogen separation with a palladium-silver membrane is described in figure 22.

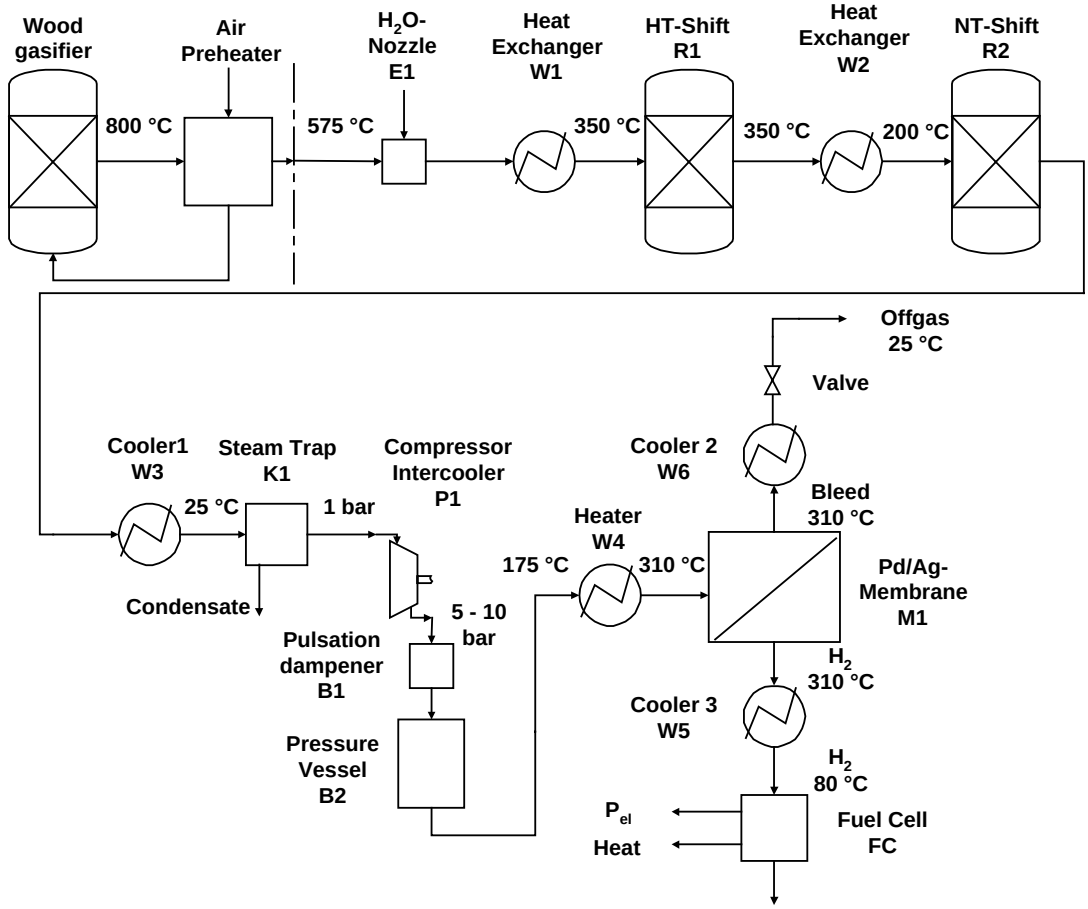

Figure 22.: Flowsheet for hydrogen separation with a palladium-silver membrane

The gasstream leaving the NT-Shift reactor is first cooled down to 25 °C. Most of the water condenses and is divided off in a steam trap. A two-stage compressor with intercooler compresses the gasstream on a suitable pressure for membrane permeation (5 - 10 bar). First the high-pressure gasstream is fed into a pulsation dampener and stored in a pressure vessel. Then the gasstream is heated up with the offgas, which does not permeate through the membrane, on the operation temperature of 310 °C. The palladium-silver membrane is permeable exclusevely for hydrogen. That means the gasstream is separated into a high purity hydrogen stream, which is suitable for a PEM-Fuel Cell, and into the offgas stream, which is used for preheating in a gas burner. The amount of hydrogen passing through the membrane depends on the difference between the hydrogen partial pressure before and behind the membrane. This is expressed by the recovery rate R_{max}, which is described by the equation

$$R_{max} = \frac{p_{Feed} \cdot x_{Feed,H2} - p_{Pure,H2}}{(p_{Feed} - p_{Pure}) \cdot x_{Feed,H2}} \quad .$$

In table 19 the gas characteristics behind the membrane are shown.

	Case I	Case II	Case III	Case IV
	moist biomass no air preheating	**moist biomass air preheating**	**dry biomass no air preheating**	**dry biomass air preheating**
Total volume flow [m^3/h]	2500,5	2738,0	2689,2	2912,0
Total mass flow [kg/h]	170,7	187,0	184,0	199,0
Total mole flow [kmol/h]	84,681	92,748	91,232	98,644
Feed pressure *before membrane* [bar]	10	10	10	10
H_2-pressure *behind membrane* [bar]	1	1	1	1
Temperature [°C]	310	310	310	310
H_2 [%]	**32,5**	**35,1**	**34,6**	**37,0**
before membrane [kmol/h]	110,089	116,723	115,484	121,663
Recovery rate R_{max}[%]	76,92	79,46	79,00	81,08
H_2 [%]	**100**	**100**	**100**	**100**
behind membrane [kmol/h]	84,681	92,748	91,232	98,644
Fuel Capacity H_2 *behind membrane* [MW]	5,688	6,230	6,128	6,626

Table 19.: Results of the gas characteristics behind the palladium-silver membrane

Because of the high-purity hydrogen the assumption of 50 % efficiency for the fuel cell is valid. The total efficiency of the whole process amounts nearly 19 to 24 %, including the gasification. The highest efficiency of 24 % appears for the case of biomass drying and air preheating. That means an electric performance of 2,4 MW is given, if 10 MW biomass input is fed into the gasifier. For the case of no-drying and no-preheating the energy output amounts only 1,91 MW. The results are shown in table 20.

	Case I	Case II	Case III	Case IV
	moist biomass no air preheating	**moist biomass air preheating**	**dry biomass no air preheating**	**dry biomass air preheating**
Fuel Capacity ($\dot{m}_B \cdot H_{u,H2}$) *before membrane* [kW]	7395	7841	7757	8172
Fuel Capacity ($\dot{m}_B \cdot H_{u,H2}$) *behind membrane* [kW]	5688	6230	6128	6626
Net Duty Compressor P_t [kW]	+ 938	+ 923	+ 926	+ 911
Heat Exchanger W4 $\dot{m}_B$ [kW]	+ 417	+ 412	+ 413	+ 407
Offgas-combustion $\dot{m}_B$ [kW]	- 417	- 412	- 413	- 407
Total Efficiency Gasification η_V [%]	73,95	78,41	77,57	81,72
Efficiency Membrane Separation $\eta_{Separation}$ [%]	76,92	79,46	79,00	81,08
Efficiency Fuel Cell η_{FC} [%]	50,00	50,00	50,00	50,00
Efficiency without internal net duty use $\eta_{ges, Membrane}$ [%]	*28,44*	*31,15*	*30,64*	*33,13*
Electric performance P_{elFC} [MW]	2,844	3,115	3,064	3,313
Internal duty requirement Compressor P_t [kW]	+ 938	+ 923	+ 926	+ 911
Efficiency internal duty requirements $\eta_{Internal}$ [%]	***67,01***	***70,37***	***69,78***	***72,50***
Overall Efficiency $\eta_{ges, Membrane}$ **[%]** ***complete process***	***19,05***	***21,92***	***21,38***	***24,01***
Overall performance P_{elM} **[MW]**	***1,905***	***2,192***	***2,138***	***2,401***

Table 20: Efficiencies for the palladium-silver membrane process

Each of the three variants also produce heat of different temperature levels and can be used for other purposes, e.g. district heating, etc.

Variants	MW therm.	°C	Source
Iron sponge reactor	0,85	120	Fluegas (0,7 MW/200°; 2,1 MW/137°C)
CO2 scrubber	2,60	80	Fuel cell (2,6 MW/80°C)
Membrane separation	4,00	80	Fuel cell (3,3 MW/80°C); Offgas (1,1 MW)

Table 21: Heat production of the processes

A good comparison of different heat and power processes is more than only to compare the efficiencies of the production of heat or of power alone. Therefore a new diagram was created as follows:

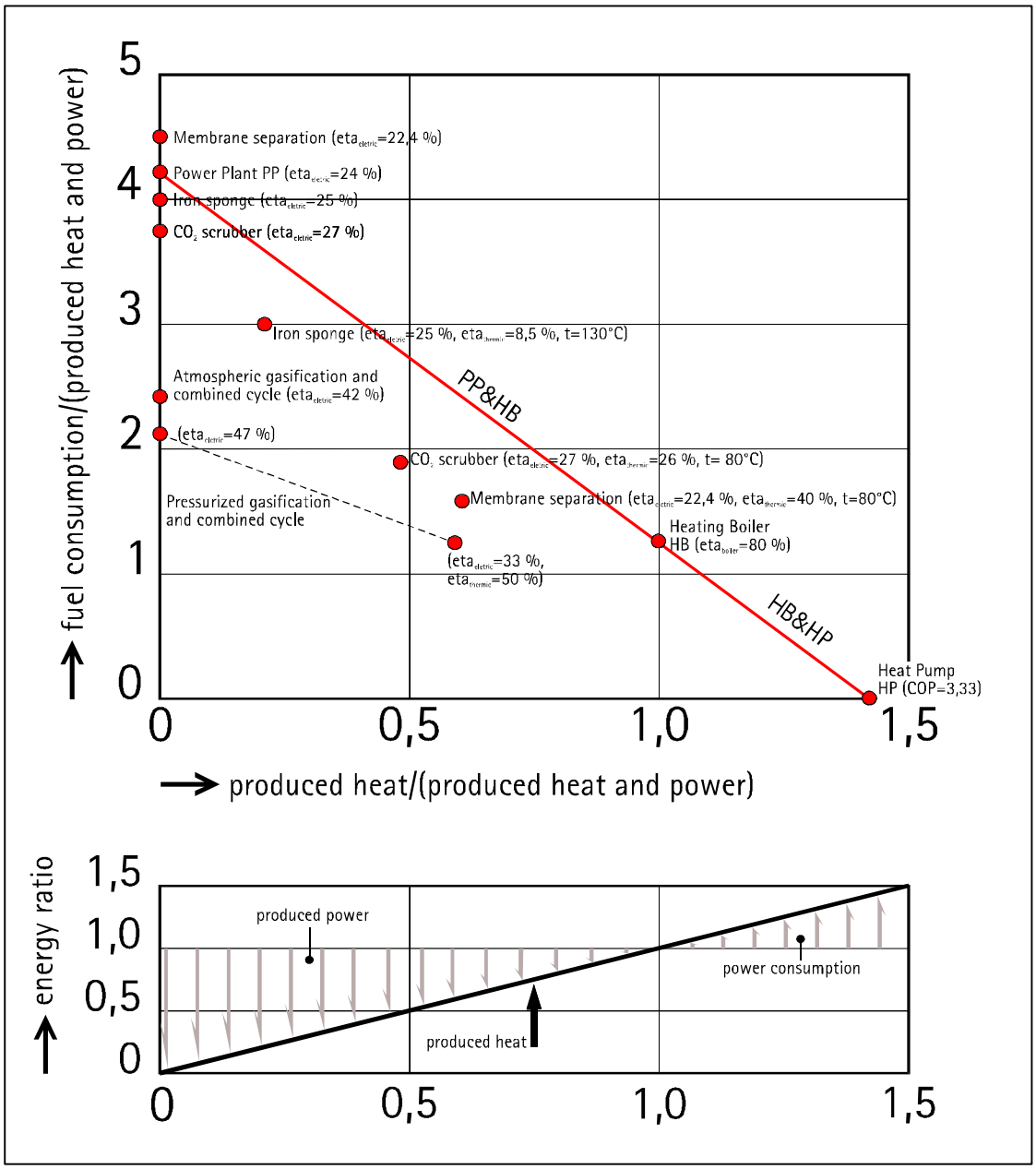

Figure 23: Efficiencies

The abscissa shows the portion of the heat produced related to the sum of heat and power production, whereas the ordinate exhibits the resulting specific fuel consumption, also based on the sum of heat and power production. A pure power plant is represented by the point PP with the coordinates x = 0; y = $1/eta_{electric}$ and a pure heating boiler by the point HB (x = 1; y = $1/eta_{boiler}$). If power and heat is provided by the mentioned stand alone plants the resulting fuel consumption is represented by the connection line of these two points. In this plot a third point should also be emphazised, the point HP which indicates a heat pump (x = COP/COP-1; y = 0 with COP coefficient of performance). Using the fuel consumption of a biomass fuelled steam cycle power plant, of a biomass fuelled heating boiler plant and the performance coefficient of a common heat pump (3 to 4) and anticipating the mixed production from these systems, one will get a single straight and declined line. This line represents the fuel consumption of the mixed or combined heat and power production according to today‘s available technology. To be better than the state of the art in regard to fuel consumption new systems have to lie blow this line.

The electric efficiencies of the investigated processes vary between 22,4 % (membrane separation) and 27,0 % (CO2 scrubber) always under the assumption of dry biomass and air preheating. For the membrane separation no heat can be used externally. In the case of the iron sponge process the electric efficiency is only 25 % but the temperature of the off gas out of the iron sponge reactor (200°C) and that of the fuel cell (137°C) offers the possibility to use the heat for external purposes like district heating.

For each process the cost have been estimated and compared to other biomass-to-energy conversion processes like combustion and steam cycle and different sorts of gasification and combined cycle.

Process	Investment costs in Euro/MWelectric	Investment costs in Euro/MWthermic
Combustion and steam cycle	4,1 – 8,6 Mio	1,0 – 2,1 Mio (eta = 24 %)
Atmospheric Gasification and combined cycle	4,9 – 7,1 Mio	2,1 – 3,0 Mio (eta = 42 %)
Pressurised Gasification and combined cycle	4,9 – 7,1 Mio	2,3 – 3,9 Mio (eta = 47 %)
Iron sponge process	12,8 Mio	3,2 Mio (eta = 25,0 %)
CO2 scrubber	10 Mio	2,7 Mio(eta = 27,0 %)
Membrane separation	21 Mio	4,7 Mio (eta = 22,4 %)

Table 22: Specific Costs

It can be seen that three processes which have been investigated have higher specific costs than comparable conventional processes at this moment. But in the future it can be expected that the costs for fuel cells will drastically decrease. Assuming that the costs for the fuel cell are approximately ½ of the total costs for the SIR and CO2 scrubber process and 1/3 for the membrane process a significant reduction could thus be achieved. Furthermore it should also be emphasised that each of the processes investigated in this study also has some important advantages but also disadvantages compared to conventional techniques.

The final table shows the main advantages and disadvantages.

Process	Plus	Minus
Iron sponge	Removal of dust, tar and H2S; Only one operation step; Low cost; Heat at 200°; no residues; Material can be recycled; SOFC at same temperature (800°); high quality of H2	high H2O content in H2 gas; discontinuous process (batch); 4 MW have to be burned => emissions
CO2 scrubber	Established technique; Continuous process; H2S can be removed; Best for PEM (80°); Internal use of heat	Complex process; Heat at low temperature level; Catalysts are waste; 2,7 MW have to be burned => emissions
Membrane separation	High purity; Continuous process; Best for PEM (80°)	Complex process; Power for compressing Heat at low temperature level; 1,5 MW have to be burned => emissions

Table 23: Advantages and disadvantages

5. Results and conclusions

The availability of biomass in Austria is sufficient to supply wood to a 10 MW gasification plant at several sites and to ensure its continuous operation. From the technical point of view, the gas clean-up is the most difficult task. The experimental investigations have shown positive results, all purification steps from catalytic tar removal to generation of pure hydrogen by the Palladium membrane separation process can be realised. However, the investigations so far have been carried out under laboratory conditions. Important additional information is expected for experiments with real gasifier gas. Except for the Palladium membrane, the cost of the plants for gas purification are quite low, compared to the cost of the fuel cell and the gasifier according to the today's state of the art.

For the combination of an air blown fluidized bed gasification, sponge iron process and SOFC as well for the complete purification chain and operation of a PEMFC, an electrical efficiency of approximately 25 % has been calculated. The biggest influence on this value is not caused by the purification processes, but by the fuel cell efficiency, which was assumed to be 50% with pure hydrogen and 37,5 % for a fuel with a low hydrogen content due to a gas utilisation of 75%. The gasifier efficiency ranges from 74 to 82%, so the best efficiency value without energy losses for gas clean-up is 30,75%.

6. Exploitation plans and anticipated benefits

The partners of the project intend to carry out future research projects on biomass related projects in order to further promote this interesting technology. As there are still a lot of tasks to solve, the transfer into a technical application will still take some time. The application of the gained knowledge in future projects is described in topic 7.

The anticipated benefits of the usage of biomass as a fuel are well known, they include environmental advantages and job creation in agriculture and industry. If additionally an emission-free conversion technology like fuel cells can be combined with biomass gasification, a very clean process of electricity and heat generation can be realised.

7. Potential applications

As the project is a kind of experimental feasibility study, a preliminary evaluation of gas purification processes in lab scale experiments has been done so far. The next step towards application would be to test the processes with real gasifier gas. This is especially important for the sponge iron process and the catalytic tar removal.

For the sponge iron process, ageing effects and lifetime of the catalysts should be investigated with real gas compositions. Another result of such investigations is the potential for gas clean-up by the sponge iron bed, possibly this bed could be used to remove dust and tars, too.

For the catalytic tar removal, poisoning effects by components in a real gas are also important. As the removal of dust was not experimentally investigated in this project, future work should focus on a suitable combination of dust and tar removal at high temperature.

For all catalytic and fine purification processes, traces of additional impurities penetrating the sponge iron reactor or the tar removal reactor like hydrogen chloride, metal compounds etc. should be considered with respect to their influence on lifetime and catalytic activity of the materials and catalysts used.